

Characteristics and sources of aerosol aminiums over the eastern coast of China: Insights from the integrated observations in a coastal city, adjacent island and the marginal seas

Shengqian Zhou¹, Haowen Li¹, Tianjiao Yang¹, Ying Chen^{*1,2}, Congrui Deng^{*1,2}, Yahui Gao^{3,4}, Changping Chen^{3,4}, Jian Xu¹

¹Shanghai Key Laboratory of Atmospheric Particle Pollution Prevention, Department of Environmental Science & Engineering, Fudan University, Jiangwan Campus, Shanghai 200438, China.

²Institute of Eco-Chongming (IEC), 3663 N. Zhongshan Rd., Shanghai 200062, China

³Key Laboratory of the Ministry of Education for Coastal and Wetland Ecosystems, School of Life Sciences, Xiamen University, Xiamen 361005, China

⁴State Key Laboratory of Marine Environmental Science, Xiamen University, Xiamen 361005, China

Correspondence: Ying Chen (yingchen@fudan.edu.cn) and Congrui Deng (congruideng@fudan.edu.cn)

Abstract. An integrated observation on aerosol aminiums was conducted in a coastal city (Shanghai) of eastern China, a nearby island (Huaniao Island) and over the Yellow Sea and East China Sea (YECS). Triethylaminium (TEAH⁺) was ~~the most~~ abundant ~~aminium observed in over~~ Shanghai but not detected over the island and the open seas, suggesting its predominantly terrestrial origin. By contrast, relatively high concentrations of dimethylaminium (DMAH⁺) and trimethylaminium+diethylaminium (TMDEAH⁺) were measured over the ocean sites, ~~indicating the significant marine source contribution~~. Environmental factors, including boundary layer height (BLH), temperature, atmospheric oxidizing capacity and relative humidity, were found to be related to aminium concentrations. All the detected aminiums demonstrated the highest levels in winter in Shanghai, consistent with the lowest BLH, ~~and~~ temperature ~~and oxidizing capacity~~ in this season. Aminiums mainly existed in fine particles and showed a bimodal distribution with two peaks at 0.18–0.32 μm and 0.56–1.0 μm , indicating that condensation and cloud processing were ~~primary/main~~ formation pathways for aminiums: ~~in analogy with NH_4^+ and non-sea-salt SO_4^{2-} (nss-SO_4^{2-})~~. Nonetheless, a unimodal distribution for aerosol aminiums was usually measured over the YECS or ~~over the Huaniao Island when~~ influenced mainly by the marine air-mass ~~over the Huaniao Island~~, which ~~was probably related to sea-spray aerosols suggested that either contained primary aminiums or provided surface for heterogeneous reactions to form secondary aminiums in marine aerosols may undergo different formation pathways from those on the land~~. Terrestrial anthropogenic sources and marine biogenic sources were both important contributors for DMAH⁺ and TMDEAH⁺, and the latter exhibited a significantly higher TMDEAH⁺ to DMAH⁺ ratio. By using the mass ratio of methanesulfonate (MSA) to ~~non-sea-salt nss-SO_4^{2-}~~ as an indicator of marine biogenic source, we estimated that marine biogenic source contributed to ~~57–83.26–31%~~ and ~~29–38.53–78%~~ of aerosol aminiums over Huaniao Island in the ~~autumn of 2016 and~~ summer of 2017 ~~and autumn of 2016~~, respectively. ~~Due to the important role of atmospheric amines in new particle formation, the estimation results highlighted the importance of marine biogenic emission of amines in the eastern coast of China, especially in summer.~~

1 Introduction

Low molecular weight amines are commonly found in the atmosphere in both ~~gaseous/gas~~ and ~~particulate/particle~~ phases (Ge et al., 2011b, a). Base on present theoretical calculations (Kurten et al., 2008; Loukonen et al., 2010; Paasonen et al., 2012; Olenius et al., 2017), laboratory simulations (Wang et al., 2010a; Wang et al., 2010b; Kurten et al., 2014; Erupe et al., 2011; Almeida et al., 2013; Yu et al., 2012) and field observations (Smith et al., 2010; Kürten et al., 2016; Tao et al., 2016), amines in the atmosphere have been proved to play an important role in new particle formation and subsequent particle growth, and thus affect both the number concentrations of aerosols and cloud condensation nuclei which are closely relevant to regional

climate (Tang et al., 2014; Yao et al., 2018). For example, dimethylamine (DMA) was found to be a key species involved in new particle formation events in the urban area of Shanghai, and the nucleation mechanism was likely to be H₂SO₄-DMA-H₂O ternary nucleation (Yao et al., 2018). Gaseous amines in the atmosphere can react with oxidants such as ·OH and O₃ to form secondary organic aerosols (SOA) (Murphy et al., 2007) or gaseous oxidation products such as imines, formamides, nitrosamines and nitramines (Nielsen et al., 2012). In aerosols, amines are mainly in the form of protonated cations, namely aminiums (Ge et al., 2011a), and the formation of aminium salts from acid-base reaction or heterogeneous reaction, such as replacing the NH₄⁺ in particles, is another important pathway for amines to form SOA in the atmosphere (Pankow, 2015; Kupiainen et al., 2012; Liu et al., 2012; Chan and Chan, 2013). In aerosols, amines are mainly in the form of protonated cations, namely aminiums (Ge et al., 2011a).

Amines originate from a wide range of sources, including anthropogenic sources such as animal husbandry and industrial emissions, as well as natural sources such as marine sources, vegetation emissions, and soil processing, ~~etc.~~ (Ge et al., 2011b; Hemmilä et al., 2018). Dawson et al. (2014) measured the concentrations of trimethylamine (TMA, 1.3–6.8 ppt) near a cattle farm which were 2–3 orders of magnitude higher than those in ambient environment. Zheng et al. (2015) measured amines in a suburban site of Nanjing in China, and concluded that amines and NH₃ in the region were mainly from industrial emissions in adjacent areas. Shen et al. (2017) demonstrated that coal combustion could emit abundant methylaminium (MMAH⁺), ethylaminium (MEA⁺) and diethylaminium (DEAH⁺) through combustion experiments, and the corresponding emission factors were 18.0±16.4, 30.1±25.6 and 14.6±10.1 mg kg(kg coal)⁻¹, respectively. In marine boundary layer, marine source is an important contributor for amines and it is/was found to be closely related to marine surface/the biological activities in ocean surface. In the North Atlantic, the concentrations of dimethylaminium (DMAH⁺) and DEAH⁺ were significantly higher during the periods with high biological activity and clean air-masses conditions than those with low biological activity or polluted air masses advecting to the sampling site, and the contributions of these two aminiums to SOA and water soluble organic nitrogen (WSO₂N) reached 11% and 35%, respectively (Facchini et al., 2008). The observation in Cape Verde also showed that the concentrations of amines aminiums were higher during the occurrence of algal blooms (Müller et al., 2009). In addition to gas-to-particle conversion which has been generally considered to be the major formation pathways (Facchini et al., 2008; Rinaldi et al., 2010), aminiums in marine boundary layer may also be generated with primary marine aerosols. For example, Fourier Transform Infrared (FTIR) spectroscopy measurements demonstrated that the submicron organic carbon was composed of 50% hydroxyl, 33% alkane and 14% amine in nascent sea spray aerosols artificially generated off the California coast (Bates et al., 2012) and of 55% hydroxyl, 32% alkane and 13% amine over the open ocean (Frossard et al., 2014). Aerosol Time-of-Flight Mass Spectrometry (ATOFMS) analyses of ambient aerosols in the Antarctic sympagic environment also indicated that 11–25% of aminiums were contributed by primary marine source (Dall'Osto et al., 2019). Previous studies on aminiums over the marginal seas of China indicated that DMAH⁺ and trimethylaminium (TMAH⁺) were overwhelmingly from marine sources (Hu et al., 2015; Yu et al., 2016; Xie et al., 2018). In May 2012, the concentrations of DMAH⁺ and TMAH⁺ over the Yellow Sea (YS) and Bohai Sea even reached 4.4±3.7 and 7.2±7.1 nmol m⁻³, which was 1–3 orders of magnitude higher than those reported in other oceanic regions (Hu et al., 2015). These extremely high concentrations were thought to be associated with high biological activities.

Given the potentially important roles of amines in the atmosphere and the complexity of their sources, it is important to conduct a systematic analysis on their concentrations, affecting factors, formation pathways and source contributions. The eastern China is a densely populated region with strong human activities and large emissions of atmospheric pollutants. Under the influence of the summer monsoon, marine source components can be vital to the atmospheric composition of the coastal area. Although the lifetime of gaseous amines in the atmosphere is only a few hours, it can be prolonged after amines partition into the particulate/particle phase, and thus, they may be transported over a long range (Nielsen et al., 2012). Many studies have been done on the atmospheric/gas and/or particle phases of amines over eastern China and adjacent seas (Huang et al., 2012;

Hu et al., 2015; Zheng et al., 2015; Huang et al., 2016; Tao et al., 2016; Yu et al., 2016; Shen et al., 2017; Xie et al., 2018; Yao et al., 2018; Yao et al., 2016). For example, C1- to C6-amines over Shanghai were measured during the summer of 2015, of which C1-, C2- and C4-amines were the dominant species with the average concentrations of 15.7, 40.0 and 15.4 ppt, respectively (Yao et al., 2016). Zheng et al. (2015) measured an average concentration 7.2 ppt of total amines in a suburban site of Nanjing during the summer of 2012, derived mainly from industrial emissions in adjacent areas. The aminiums in fine particles over Shanghai in the summer of 2013 were found to exhibited a high concentration (mean 86.4 ng m⁻³) and played an important role in the new particle formation events (Tao et al., 2016). Previous studies on aminiums over the marginal seas of China indicated that DMAH⁺ and trimethylaminium (TMAH⁺) were overwhelmingly from marine sources (Hu et al., 2015; Yu et al., 2016; Xie et al., 2018). Nonetheless, In May 2012, the concentrations of DMAH⁺ and TMAH⁺ over the Yellow Sea (YS) and Bohai Sea even reached 4.4 and 7.2 nmol m⁻³, which was 1–3 orders of magnitude higher than those reported in other oceanic regions (Hu et al., 2015). These extremely high concentrations were thought to be associated with high biological activities. In spite of these field studies, the long-term observation of aminiums over the coastal sea and quantitative estimate of the contribution of marine biogenic source to aerosol aminiums are still lacking.

In this study, the aminiums over a coastal megacity (Shanghai), a nearby island (Huaniao Island) and marginal seas (the Yellow Sea and East China Sea, YECS) were measured. The relationships between aminium concentrations and environmental factors were systematically analyzed. The size distributions of aminiums were investigated with the speculation of primary main formation pathways. Besides, the dominant sources determining the concentrations and ratios between aminium species were elucidated, and the contributions of terrestrial anthropogenic and marine biogenic sources to aminiums were quantitatively estimated. Our results will be a great help for understanding the chemical properties, reaction pathways and sources of aerosol aminiums over the coastal area and the ocean.

2 Sampling and Analysis

2.1 Aerosol sampling

The sampling site in Shanghai was located on top of the No.4 teaching building of Fudan University (31.30° N, 121.50° E) (Fig. 1). This site is affected by the school, residential, commercial and traffic activities and can be representative of coastal cities. Particulate matters with an aerodynamic diameter less than 2.5 μm (PM_{2.5}) were simultaneously collected by two medium-flow samplers (100 L min⁻¹, HY-120B, Hengyuan) using a 90 mm pre-combusted quartz filter (Whatman) and a cellulose filter (Grade 41, Whatman), respectively. A total of 131 samples were collected within four seasons with the sampling duration ~24 hours around 24 hours (spring: 25 Mar. – 26 Apr., 2013; summer: 16 Jul. – 17 Aug., 2013; autumn: 30 Oct. – 30 Nov., 2013; winter: 1 Dec., 2013 – 23 Jan., 2014) (Table 1).

Aerosols were also collected at Huaniao Island (HNI, 30.86° N, 121.67° E) which was about 80 km away from Shanghai in the East China Sea (ECS) (Fig. 1). The locally anthropogenic emissions were negligible, but the site was affected by the terrestrial transport and the ship emission from nearby container ports (Wang et al., 2016; Wang et al., 2018). Fourteen-PM_{2.5} samples were collected in the summer of 2016 (4 Aug. – 18 Aug.) and size-segregated samples were obtained using a 10-stage Micro-Orifice Uniform Deposit Impactor (30 L min⁻¹, MOUDI, MSP Model 110-NR) and 47 mm PTFE filters (Zeflour, PALL) between in the autumn of 2016 fall (12 Nov. – 3 Dec.), the spring of 2017 (11 Mar. – 19 Mar.) and 2017-the early and late summer of 2017 (22 Jun. – 9 Jul. and 27 Aug. – 12 Sep., respectively) (Table 1). The 50% cutoff diameters for 10 stages were 18, 10, 5.6, 3.2, 1.8, 1.0, 0.56, 0.32, 0.18, 0.10 and 0.056 μm, and the sampling durations were 24–48 hours.

The size-segregated samples were also collected over the YECS onboard research vessel (R/V) *Dong Fang Hong II* in the spring of 2017. The cruise started from Qingdao on March 27 and returned on April 15 (Fig. 1), and a total of 9 sets of samples were obtained.

2.2 Chemical analysis

One fourth of PM_{2.5} sample and half of MOUDI sample filters were cut and placed into a polypropylene jar (Nelgene) with 15 mL and 20 mL of ultrapure water (18.25 MΩ cm⁻¹) respectively for 40 min ultrasonic extraction. The extract was filtered through a 0.45 μm PTFE filter (Jinteng) and stored at 4 °C for ion measurement. Ion Chromatograph (DIONEX ICS-3000, Thermo-Fisher) assembled with AG11-HC and AS11-HC was used to determine anions including Cl⁻, NO₃⁻, SO₄²⁻, HCOO⁻, methanesulfonate (MSA), malonate, succinate, glutarate, maleate and C₂O₄²⁻. The columns CG17 and CS17 were used to measure inorganic cations including Na⁺, NH₄⁺, K⁺, Mg²⁺ and Ca²⁺ and aminiums. ~~The detailed procedures for measuring Six aminiums including DMAH⁺, TMAH⁺+DEAH⁺, propylaminium (MPAH⁺), triethylaminium (TEAH⁺), ethanolaminium (MEOAH⁺) and triethanolaminium (TEOAH⁺) refer to Zhou et al. (2018).~~ could be effectively separated and measured using the IC method. ~~The MMAH⁺ and MEAH⁺ in the aerosols could not be quantified because their peaks were obscured by the wide and distorted peak of NH₄⁺.~~ It should be noted that TMAH⁺ and DEAH⁺ could not be completely separated using the IC system (VandenBoer et al., 2012; VandenBoer et al., 2011; Zhou et al., 2018; Huang et al., 2014). ~~Nonetheless~~ Therefore, the sum of TMAH⁺ and DEAH⁺ concentrations (referred to named as TMDEAH⁺) might be were quantified using the calibration curve of TMAH⁺ with errors less than 3% (Zhou et al., 2018). ~~With the sampling volumes of 144 and 86 m³ for PM_{2.5} and MOUDI samples respectively, the detection limits of DMAH⁺, TMDEAH⁺, TEAH⁺, MPAH⁺, MEOAH⁺ and TEOAH⁺ were 0.55, 0.78, 1.93, 2.59, 1.94 and 4.96 ng m⁻³ for PM_{2.5} samples and 0.20, 0.29, 0.71, 0.95, 0.56 and 1.82 ng m⁻³ for samples collected in each MOUDI stage. MPAH⁺, MEOAH⁺ and TEOAH⁺ were rarely detected in the aerosol samples (<10%) and thereby not reported in this study. The detailed information about analysis of aminiums were given in Zhou et al. (2018).~~

One fourth of PM_{2.5} cellulose sample filter was cut and digested with 7 mL of HNO₃ and 1 mL of HF (both acids were purified from GR using a sub-boiling system) at 185 °C for 30 min in a microwave digestion system (MARS5 Xpress, CEM). An Inductively Coupled Plasma Optical Emission Spectroscopy (ICP-OES, SPECTRO) was used for determining elements Al, Ca, Fe, Na, P, S, Cu, K, Mg, Mn, Zn, As, Ba, Cd, Ce, Co, Cr, Mo, Ni, Pb, Ti, and V. The detailed procedures refer to Wang et al. (2016).

2.3 Auxiliary data

The 3-hour resolution meteorological data of Baoshan station in Shanghai (WMO index: 58362) were obtained from the National Climatic Data Center (NCDC, <https://www.ncdc.noaa.gov/isd>). The 10-second resolution meteorological data were recorded by a shipborne meteorological station during the cruise. The planetary boundary layer height (BLH) and 6-hour accumulated precipitation (TPP6) ~~for the cruise~~ were extracted from NCEP's Global Data Assimilation System Data (GDAS). The daily concentrations of gaseous pollutants (SO₂, CO, NO₂ and O₃) ~~in averaged from 9 real-time monitoring stations of Shanghai~~ were obtained from the Shanghai Environmental Monitoring Center (<http://www.semc.gov.cn/aqi/home/DayData.aspx>). Three-day air mass backward trajectories were calculated using a Hybrid Single-Particle Lagrangian Integrated Trajectory (HYSPLIT) model (<http://ready.arl.noaa.gov/HYSPLIT.php>) with the starting height at 100 meters.

3 Results and discussion

3.1 Seasonal and spatial variations of aminium concentrations

~~The mean concentrations of NH₄⁺ and aminiums in each campaign of this study and reported in literatures were listed in Table 2. It should be noted that TEAH⁺ concentrations over Huaniao Island and the YECS were mostly below the detection limits (<DL). For other aminiums and TEAH⁺ over Shanghai, the number of samples below detection limits were generally less than 30%. These undetectable concentrations were considered to be zero for the calculation of means and standard deviations. Three~~

aminiums, DMAH⁺, TMDEAH⁺ and TEAH⁺, were commonly detected in the aerosol samples collected from Shanghai. The most abundant aminiums were DMAH⁺ and TEAH⁺ with their annual means of 15.6 and 16.0 ng m⁻³, respectively. By comparison, the average TMDEAH⁺ concentration (4.4 ng m⁻³) was significantly lower. All three aminiums showed the highest concentrations in winter and the lowest levels in spring (DMAH⁺) and summer (TMDEAH⁺ and TEAH⁺), which generally agreed with the seasonal trends of PM_{2.5} and NH₄⁺ concentrations in Shanghai (Figure 2). Specifically, the average TEAH⁺ reached 35.2 ng m⁻³ in winter in Shanghai, about 40 times as much as that in summer. ~~By contrast,~~ TEAH⁺ was mostly below the detection limit in the aerosols collected over Huaniao Island and the YECS, suggesting its dominant land sources and negligible marine contribution. ~~Differently~~By contrast, the average DMAH⁺ and TMDEAH⁺ concentrations (14.0 and 13.2 ng m⁻³) over Huaniao Island were close to and significantly higher than those ~~of over~~ Shanghai, respectively. Similarly high concentrations of DMAH⁺ and TMDEAH⁺ (11.9 and 14.6 ng m⁻³) were also observed over the YECS (Fig. 2 and Table 2), suggesting that the two aminiums might have notable marine sources. Accordingly, both species reached the highest levels during the summer campaigns in 2017 at Huaniao Island, consistent with the highest primary productivity in the coastal ECS and prevailing winds from the ocean in summer. As a major component of fine particles over eastern China with similar chemical properties to aminiums, NH₄⁺ was mainly from terrestrial sources and its concentrations over Huaniao Island ~~and~~ YECS were much lower than those over Shanghai (Fig. 2).
 Our measurement of DMAH⁺ in Shanghai was comparable to those previously reported from the urban sites ~~(Table 2)~~, but generally higher than those measured in the forest areas of Toronto (VandenBoer et al., 2012), Hyytiälä (Hemmilä et al., 2018) and Guangdong (Liu et al., 2018a). This implies that anthropogenic activities may be crucial sources of DMAH⁺ in the urban atmosphere. The TMDEAH⁺ concentrations in our study were much lower than those reported by Tao et al. (2016) in Shanghai. Their sampling location was close to the residential areas and could be influenced by the local sources such as human excreta emission (Zhou et al., 2018). The aerosol TEAH⁺ concentrations in China were ~~firstly reported in our study and could not be compared to previous work. Except for the three aminiums reported in our study for the first time and could not be compared to previous work. According to previous measurement results for gaseous amines in the same site from July 25 to August 25 in 2015, the average mass concentrations of C2-, C3- plus C4-, and C6-amines were 80.4, 53.1 and 15.8 ng m⁻³, respectively (Yao et al., 2016). The order of concentrations was consistent with that of the corresponding aerosol aminiums in the summer of 2013 which was DMAH⁺ > TMDEAH⁺ > TEAH⁺ (9.1, 1.7 and 0.9 ng m⁻³, respectively) in this study. Based on these concentrations, the ratios of each amine vs. aminium were roughly calculated and C2-amines/DMAH⁺, (C3- plus C4- amines)/TMDEAH⁺ and C6-amines/TEAH⁺ were 8.8, 30.1 and 17.9, respectively. These values were comparable to the ratio of total amines to total aminiums (14.9) over a mountain site in southern China (Liu et al., 2018a). Except for the three aminiums commonly detected in this study, MMAH⁺ and MEAH⁺ (Liu et al., 2018a; Ho et al., 2015; Shen et al., 2017) were~~ other abundant aminiums detected in the urban site.
 Aerosols were ~~sampled~~collected using a MOUDI over Huaniao Island and the YECS. Aminiums in PM_{1.8} of the MOUDI samples were compared to those of PM_{2.5}, since MOUDI does not have the 50% cutoff diameter of 2.5 µm and aminiums in PM_{1.8} accounted for over 60% concentrations of the whole size range of aerosols. Our measurements of aminiums over Huaniao Island and the YECS were comparable to those previously observed over the eastern China seas (Hu et al., 2015; Yu et al., 2016; Xie et al., 2018), but they were apparently higher than many other oceanic regions such as Arabian Sea (Gibb et al., 1999) and Cape Verde (Müller et al., 2009). The high aminiums over the YECS were probably associated with the severe air pollution in eastern China as well as the high ocean productivity in marginal seas.

3.2 Environmental factors affecting aminium concentrations

3.2.1 Boundary layer height (BLH)

The concentrations of PM_{2.5}, NH₄⁺ and three aminiums sampled in Shanghai in 2013 dropped significantly when the BLH

increased from 200 m to 500 m and then slowly decreased with the further increase of BLH (Fig. 3a and Fig. S1), due to the improvement of diffusion condition enhanced ventilation. Specifically, the concentrations of DMAH⁺, TMDEAH⁺ and TEAH⁺ (58.4, 13.9 and 80.5 ng m⁻³) in Shanghai reached the maximum along with PM_{2.5} (447 μg m⁻³) during the severe haze event between 30 Nov. and 8 Dec. 2013, when the average BLH and wind speed were 298 m and 1.35 m s⁻¹, respectively (Fig. S2). By comparison, the average concentrations of DMAH⁺, TMDEAH⁺ and TEAH⁺ (8.9, 4.0 and 10.1 ng m⁻³) were much lower prior to the haze event (on 26–29 Nov 2018) associated with the higher BLH (636.4 m) and wind speed (2.73 m s⁻¹). Thus, the generally poor diffusion condition stagnant meteorology in winter (Liu et al., 2013) could cause a substantial increase accumulation of aerosol aminiums in aerosols and lead to the seasonal variation of aminiums in Shanghai.

3.2.2 Temperature

To eliminate the synchronous change of aminiums and NH₄⁺ with PM_{2.5}, the mass ratios of aminiums to PM_{2.5} (aminiums/PM_{2.5}) and NH₄⁺ to PM_{2.5} (NH₄⁺/PM_{2.5}) were applied for analysis. These ratios were found to be negatively correlated with air temperature in Shanghai (Fig. 3b). Similar to NH₄⁺, aminiums combined with NO₃⁻, Cl⁻ and organic acids are semi-volatile and can dissociate in the atmosphere (Tao and Murphy, 2018). So the negative correlations may be explained by the movement of gas-particle partitioning equilibrium to the gas phase at higher temperatures (Ge et al., 2011a). This is consistent with the previous observation that the proportion of particles containing aminiums in the urban area of Shanghai was much higher in winter (23.4%) than that in summer (4.4%) (Huang et al., 2012). The seasonal variation of temperature may also lead to the change of concentrations of aerosol aminiums. It should be pointed out that environmental variables like BLH and temperature are constantly changing with time and their impacts on aminium concentrations may vary within the sampling duration (24 or 48 hours). However, these variables must be averaged over the same time interval as aminium concentrations. This analysis may eliminate the instant discordance and improve the correlations between environmental variables and aminiums or aminiums/PM_{2.5}, and the results could well explain the seasonal variation of aminiums.

3.2.3 Oxidizing capacity

As gaseous amines can be oxidized by oxidants such as ·OH, O₃ and NO₃· in the atmosphere before partitioning into the particulate phase (Ge et al., 2011b; Nielsen et al., 2012; Yu and Luo, 2014), aminium concentrations in aerosols may decrease with the enhanced atmospheric oxidizing capacity. Ozone concentration can represent oxidizing capacity of the lower atmosphere (Thompson, 1992). Here the relationship between aminium/NH₄⁺ ratios and O₃ was examined, because the formation of particulate aminiums and NH₄⁺ were both temperature-dependent and using their ratios could avoid the temperature effect to some extent. Besides, the residence time of NH₃ in the atmosphere due to the oxidation reaction is about 72.3 days (Ge et al., 2011b), and therefore NH₄⁺ concentrations in aerosols should not be affected by O₃. A negative correlation was found between the TEAH⁺/aminiums/NH₄⁺ and O₃ concentrations in Shanghai during the summer of 2013 (Fig. 3c). Differently in other seasons, the DMAH⁺/NH₄⁺ and TMDEAH⁺/NH₄⁺ reached the highest values at the mid-level correlations were not obvious, especially in winter when O₃ concentrations were the lowest and neither of aminiums/NH₄⁺ was correlated with O₃ (Figure S3). O₃ and decreased with both low and high concentrations of O₃. This verifies In general, atmospheric oxidizing capacity is the strongest in summer (Logan, 1985; Liu et al., 2010), and the results verified that high oxidizing capacity in summer may reduce the formation of particulate aminiums by oxidizing gaseous amines. It was consistent with the diurnal pattern of gaseous amines with the lowest values at noon and the negative correlations between the concentrations of amines and O₃ observed in Shanghai during the summer of 2015 (Yao et al., 2016). It should be noted that there was no significant variation in temperature and little rainfall during the sampling periods in the summer of 2013. In other seasons, due to the relatively weak photochemistry and more complex sources and meteorology, other factors except oxidizing capacity played more important roles in affecting aerosol aminiums. This also implies that DMAH⁺ and TMDEAH⁺ may have the sources different from TEAH⁺ but similar to O₃ precursors such as biogenic VOCs. Among the three

amines, the rate constants of TEA reacting with $\cdot\text{OH}$ and O_3 were larger than those of other two amines (Nielsen et al., 2012), and thereby TEAH⁺ showed the most significant correlation with O_3 . In general, atmospheric oxidizing capacity was the strongest in summer (Logan, 1985; Liu et al., 2010), which could be another reason for seasonal variation of aerosol aminiums in Shanghai.

In the spring of 2017 over the YECS, the concentrations of DMAH⁺ and TMDEAH⁺ were found to be the lowest between 29 Mar and 4 Apr when it was sunny and Chl-a concentrations were relatively low. The relatively low biogenic emission may partly account for the low level aminiums. Nonetheless, the HCOO⁻ in aerosols, a product of photochemical reactions under high oxidizing capacity (Souza, 1999; Tsai et al., 2013), reached the highest level between 31 Mar. and 4 Apr. (42.1–55.5 ng m⁻³). Its concentrations were inversely correlated with aminiums when eliminating the lowest values of HCOO⁻ (Fig. 4). This further suggests that high oxidizing capacity may be one of causes for lowered aminiums in marine aerosols.

3.2.4 Relative humidity and fog processing

In the spring of 2017 over the YECS, although the sample of 4–5 Apr. was influenced by high Chl-a concentrations and low BLH, the concentrations of DMAH⁺ and TMDEAH⁺ (13.3 and 17.4 ng m⁻³) were about half of those on 7–9 Apr. (Fig. S4). This was probably due to the intense fog event occurred on 7–9 Apr. with relative humidity > 90%, which could enhance the gas-to-particle partitioning of amines. The enhancement of TMA gas to particles by cloud and fog processing has been observed in both field and laboratory simulations (Rehbein et al., 2011). It was also found that the number fraction of TMA-containing particles dramatically increased from ~7% in clear days to ~35% in foggy days and number-based size distribution of TMA-containing particles shifted towards larger mode, peaking at the droplet mode (0.5–1.2 μm) in Guangzhou (Zhang et al., 2012). The investigation over the Yellow and Bohai seas in the summer of 2015 found significantly positive correlations between the concentrations of DMAH⁺ and TMAH⁺ and relative humidity (Yu et al., 2016). Therefore, fog and high relative humidity (RH) are also favorable conditions for gas-to-particle conversion of amines, high relative humidity and fog event may lead to an increase of aminiums in marine aerosols.

3.3 Size distributions and formation pathways of aerosol aminiums

The aminiums were mainly distributed in fine aerosols with diameter less than 1.8 μm , and the mass percentages of DMAH⁺ and TMDEAH⁺ in the coarse mode were around 36% in the autumn of 2016 at Huaniao Island and less than 15% in all other campaigns at Huaniao Island and over the YECS (Fig. 6a–d, S4a–d). This is consistent with the previous reports that >70% of aminiums were distributed in fine particles over Shanghai during the summer of 2013 (Tao et al., 2016) and over the western North Pacific and its marginal seas (Xie et al., 2018). The aminiums mostly demonstrated a bimodal distribution in the autumn and early summer campaigns at Huaniao Island with peaks at 0.18–0.32 μm (condensation mode) and 0.56–1.0 μm (droplet mode). This is similar to the size distributions of DMAH⁺ and TMDEAH⁺ observed in Shanghai (Tao et al., 2016) and to NH₄⁺ and non-sea-salt (nss-SO₄²⁻) in all campaigns over Huaniao Island and the YECS (Fig. S3–S4–5). The size distribution suggests that the gas-to-particle condensation (condensation mode) and cloud processing (droplet mode) seem to be primary major mechanisms for the formation of aminiums and other secondary species NH₄⁺ and nss-SO₄²⁻.

In order to compare the contributions between condensation and cloud processing to the formation of specific species, the ratio of its concentrations in droplet mode (0.56–1.0 μm) to condensation mode (0.18–0.32 μm) was calculated (denoted as α). It could be seen that the α values of NH₄⁺ and nss-SO₄²⁻ were significantly greater than 1, especially in the case of high concentrations, indicating that the cloud processing probably determined the concentrations of these species (Fig. S6). Differently, aminiums had α values around 1, suggesting that condensation and cloud processing might be equally important to the formation of aminiums.

In late summer at Huaniao Island and the spring cruise over the YECS when air masses were mainly from oceanic regions (see Sect. 3.4.3), the aminiums generally exhibited a unimodal distribution with one wide peak at 0.18–1.0 μm due to the increased

concentrations at 0.32–0.56 μm (Fig. 6e5e-h). The concentrations of NH_4^+ and nss-SO_4^{2-} also showed a significant elevation in the size range of 0.32–0.56 μm during these periods. The deviation of MOUDI cutoff diameters during the sampling could be ruled out because the concentrations of particulate matter always presented a trimodal distribution with peaks at 0.18–0.32 μm , 0.56–1.8 μm and 3.2–10 μm . The unimodal distributions of aminiums with the peak at 0.18–1.0 μm have been widely reported over the eastern China seas (Hu et al., 2015; Yu et al., 2016; Xie et al., 2018). This suggests that the formation mechanisms of aerosol aminiums over the ocean may be different from that ~~in over the urban area land~~. It was indicated that the high concentration and unique size distribution of TMAH⁺ observed over the oligotrophic western North Pacific were mainly attributed to the primary TMAH⁺ in sea-spray aerosols (Hu et al., 2018). ~~In addition, some studies have demonstrated that artificially generated sea spray aerosols and actual primary marine aerosol both contained amines/aminiums (Bates et al., 2012; Frossard et al., 2014; Dall'Osto et al., 2019).~~ So we speculate that the elevated concentrations of aminiums at 0.32–0.56 μm over the eastern China seas may be also associated with the increased concentration of sea-spray aerosols which contain substantial primary aminiums ~~or provide more surface for~~. ~~In other hand, the heterogeneous reactions to form formation of secondary aminiums on the surface of sea spray aerosols cannot be ruled out~~ (Yu et al., 2016).

3.4 Sources of aerosol aminiums

3.4.1 Anthropogenic sources on ~~the~~ land

Correlation analysis was carried out between aminiums, other $\text{PM}_{2.5}$ components and gaseous pollutants measured in Shanghai (Fig. 87). It can be seen that the secondary inorganic components SO_4^{2-} , NO_3^- and NH_4^+ (SNA), $\text{PM}_{2.5}$ and DMAH⁺ were significantly correlated with each other with the correlation coefficients above 0.6. This suggests that anthropogenic sources may have a great contribution to the atmospheric DMA in Shanghai, ~~which is consistent with previous findings in Nanjing (Zheng et al., 2015). Considering the unique role of DMA in new particle formation (Almeida et al., 2013), our results re-enforce that the frequent new particle formation events observed in extremely polluted Chinese cities are indeed, at least in part, due to amines (Yao et al., 2018).~~ The correlations between TEAH⁺ and SNA were relatively weak, but TEAH⁺ was found to be significantly correlated with the components mainly from industrial sources (represented by the high concentrations of K, Mn, Cd, Pb, Zn, and Cl⁻) (Tian et al., 2015; Liu et al., 2018b), indicating that the industrial emission could be an important source of TEA. ~~It was consistent with the observation result in a suburban site that gaseous C4- to C6-amines had some abrupt and frequent increase in the night and may be caused by some local emissions (You et al., 2014).~~ Compared to the DMAH⁺ and TEAH⁺, TMDEAH⁺ showed much weaker correlations with the anthropogenically derived components. Weak correlations were also found between all the aminiums and V, Ni, Al, Mg, Ca and Fe, suggesting that ship emission (traced by V and Ni) and soil dust (represented by Al, Ca and Fe) were not main sources of aminiums in $\text{PM}_{2.5}$ over Shanghai.

3.4.2 Marine biogenic source

As discussed in Sect. 3.1, the relatively high concentrations of DMAH⁺ and TMDEAH⁺ over Huaniao Island and the YECS implied that the marine sources contributed substantially to these two aminiums. Accordingly, a spatial variation of aminium concentrations was observed over the YECS during the spring cruise. The concentrations of DMAH⁺ and TMDEAH⁺ increased by a ~~foldfactor~~ of 3–5 in the southern ECS (average 24.4 and 40.3 ng m^{-3} for the samples of 7–11 Apr. respectively) compared to the YS and northern ECS (average 7.0 and 8.4 ng m^{-3} for the samples of 27 Mar.–5 Apr. respectively) (Fig. 98). This is consistent with the noticeable difference of Chl-a concentrations between the southern and northern YECS (2.3 ~~foldstimes~~ higher in southern YECS than that in northern YECS, unpublished data). Furthermore, the highest TMDEAH⁺ and lowest NH_4^+ concentrations observed on 7–11 Apr. corresponded to the air-mass back trajectories originating from the ocean, suggesting that the metabolic activities of surface plankton in the high-productive seas could be a strong source of amines as previously reported (Facchini et al., 2008; Müller et al., 2009; Sorooshian et al., 2009; Hu et al., 2015). Differently, the high

concentrations of aminiums observed on 14 Apr. near Qingdao was affected by the air masses transported from eastern China (Fig. 98) and thereby contributed mainly by terrestrial sources.

Fine-mode NH_4NO_3 could decompose during its transport from the land to the ocean, and the released HNO_3 gas would react with dust and sea salt aerosols to form coarse-mode NO_3^- . Therefore, negative correlations were observed between the concentrations of fine-mode NO_3^- and alkaline species ($\text{Na}^+ + \text{Ca}^{2+}$) over the East Asia (Bian et al., 2014; Uno et al., 2017). Since only one dust event was encountered on 12–13 Apr. during the cruise (unpublished data), the coarse-mode NO_3^- in this study should be mostly formed by the heterogeneous reaction with sea salts. Therefore, the importance of terrestrial transport to marine aerosols could be roughly estimated by the percentage of NO_3^- in the fine mode. For aerosols collected on 29–31 Mar., 4–5 Apr., 7–9 Apr. and 9–11 Apr., over 2/3 concentrations of NO_3^- were in the coarse mode ($>1.8 \mu\text{m}$, Fig. 10a9a). These samples should be less affected by the terrestrial air masses (referred to category 1) compared to other samples (referred to category 2), and the judgment analysis was consistent with the pointing forward directions of backairmass trajectories (Fig. S5S6). Aminiums were negatively correlated with NH_4^+ for Category 1 samples suggesting that aminiums were probably dominated by marine biogenic sources whereas NH_4^+ was influenced by terrestrial transport (Fig. 10b9b). For Category 2 samples, a positive correlation was found between aminiums and NH_4^+ , indicating that terrestrial sources could contribute significantly to aminiums over the YECS in these cases (Fig. 10e9c).

3.4.3 Source contributions to aminiums over the coastal sea

Huaniao Island is located in the frontline of terrestrial transport to the ECS and influenced by the air masses from the land or ocean depending on the seasonal variation of prevailing winds. Significantly positive correlations were found between the concentrations of aminiums and NH_4^+ in the autumn but not in the summer of 2016 or in late summer of 2017 (Fig. 4410). Accordingly, the majority of backward trajectories pointed to the northern China in autumn whereas air masses predominantly originated from the ECS in summer (Fig. 4211). Meanwhile, NO_3^- demonstrated a tri-modal distribution with three peaks at $0.18\text{--}0.32 \mu\text{m}$ (condensation mode), $0.56\text{--}1.0 \mu\text{m}$ (droplet mode) and $3.2\text{--}5.6 \mu\text{m}$ (coarse mode) in autumn but only one peak at $3.2\text{--}5.6 \mu\text{m}$ in late summer of 2017 (Fig. S6S7). These implies that terrestrial transport could be a dominant source for aminiums over the coastal ECS in autumn while marine sources were dominant in late summer. In early summer of 2017, the mass ratios of aminiums to NH_4^+ were significantly lower on 26–28 Jun. than those on other days (Fig. S7S8), corresponding to different origins and properties of the air masses. Removing the data measured on 26–28 Jun., we found a significantly positive correlation between the concentrations of DMAH^+ and NH_4^+ but not between TMDEAH^+ and NH_4^+ . This suggests that DMAH^+ and TMDEAH^+ may be predominantly derived from terrestrial and marine sources, respectively.

Good positive correlations were generally found between the concentrations of TMDEAH^+ and DMAH^+ over Huaniao Island and the YECS, and the slope for autumn samples dominated by terrestrial sources was significantly lower than those influenced primarily by marine air masses (e.g. late summer at Huaniao Island and spring over the YECS, Fig. 4312). The highest slope of TMDEAH^+ vs. DMAH^+ (1.98) occurred in the summer of 2016 which was also mainly affected by marine sources. Therefore, it is speculated that aminiums derived from marine biogenic source might have significantly higher TMDEAH^+ to DMAH^+ ratios than those from terrestrial sources. Similarly, Hu et al. (2015) observed a significant correlation between the TMDEAH^+ and DMAH^+ concentrations over the Yellow Sea with the slope of 1.27–2.49. In early summer of 2017, the weak correlation between the DMAH^+ and TMDEAH^+ and very low slope (0.29) suggested the mixing of terrestrial and marine influence on aminiums over Huaniao Island during that period as discussed above.

The dimethylsulfide (DMS) produced in seawater by the metabolism of plankton will be released into the atmosphere, and SO_2 , MSA, SO_4^{2-} and other products can be formed through a series of oxidation reactions (Saltzman et al., 1985; Charlson et al., 1987; Faloona, 2009; Barnes et al., 2006). MSA is often used as a tracer of marine biogenic source to calculate the marine biogenic contribution to nss-SO_4^{2-} (Yang et al., 2009; Yang et al., 2015). Therefore, the mass ratio of MSA to nss-SO_4^{2-} ($\text{MSA}/\text{nss-SO}_4^{2-}$) can be used to indicate the contribution of marine sources to relevant aerosol components. A

significantly linear relationship was found between aminium/ NH_4^+ and $\text{MSA}/\text{nss-SO}_4^{2-}$ for the samples collected in the autumn of 2016 and summer of 2017 over Huaniao Island (Fig. 4413). The value of aminium/ NH_4^+ increased with the increasing contribution of marine sources to the aerosol aminium. When the marine biogenic source contribution is 0, the corresponding aminium/ NH_4^+ values (b in Eq. (3)) represent the average ratios completely contributed by terrestrial sources. By multiplying the ratios by NH_4^+ concentrations, the aerosol aminiums contributed by terrestrial sources can be calculated (Eq. (4)). Therefore, the contributions of terrestrial and marine sources to aerosol aminiums can be quantitatively estimated.

$$([\text{aminium}]/[\text{NH}_4^+])_{\text{terrestrial}} = k \times ([\text{MSA}]/[\text{nss} - \text{SO}_4^{2-}])_{\text{terrestrial}} + b \quad (3)$$

$$[\text{aminium}] = ([\text{aminium}]/[\text{NH}_4^+])_{\text{terrestrial}} \times [\text{NH}_4^+] + [\text{aminium}]_{\text{marine}} \quad (4)$$

where k and b are the slope and intercept of the linear fitting equation of $[\text{aminium}]/[\text{NH}_4^+]$ and $[\text{MSA}]/[\text{nss} - \text{SO}_4^{2-}]$, respectively (Fig. 4413).

Although most of MSA comes from marine sources, the terrestrial sources may also have a certain contribution (Yuan et al., 2004). Therefore, $\text{MSA}/\text{nss-SO}_4^{2-}=0$ was not used as the end member value for calculating the terrestrial contribution. In winter, due to the prevailing northwest monsoon and low marine biogenic activities at low temperature, the aerosol components over Huaniao Island were overwhelmingly affected by terrestrial transport. We conducted total suspended particles (TSP) sampling in the winters of both 2014 and 2015 and obtained a total of 41 values of $\text{MSA}/\text{nss-SO}_4^{2-}$ which were between 0.0010 and 0.0068. The smallest 5 values were considered to represent the situations completely contributed by terrestrial sources, with an average 0.0018 ± 0.0007 . We have simultaneously measured MSA and nss-SO_4^{2-} in a total of 64 total suspended particle (TSP) samples collected in the autumn of 2016 and the summer of 2017. The retention percentage of air mass over the land (R_L) was calculated for each sample based on three-day backward trajectories (Figure S9 and see supplementary text for more information). Samples with the largest 10% R_L values ($n=7$, $R_L > 74\%$) were considered to be terrestrial-dominant samples with the average $\text{MSA}/\text{nss-SO}_4^{2-}$ (± 1 standard deviation) of 0.0021 ± 0.0013 . Therefore, this value was regarded as the end member value of terrestrial $\text{MSA}/\text{nss-SO}_4^{2-}$ in these seasons. Substituting it into the previous fitting equation, the values of $([\text{DMAH}^+]/[\text{NH}_4^+])_{\text{terrestrial}}$ and $([\text{TMDEAH}^+]/[\text{NH}_4^+])_{\text{terrestrial}}$ were 0.00620068 ($0.00440038-0.00930105$) and 0.00280034 ($0.000800005-0.00520076$), respectively. Then the average contributions of terrestrial and marine sources to the two aminiums in each campaign were calculated and shown in Table 3. It can be seen that the average terrestrial contributions to DMAH^+ and TMDEAH^+ in aerosols were both more than 60% in autumn, higher than those in summer. The contributions of marine sources during late summer of 2017 ($66.563.0\%$ for DMAH^+ and $82.578.3\%$ for TMDEAH^+) were higher than those in early summer (5753.3% for DMAH^+ and $79.474.2\%$ for TMDEAH^+), which was consistent with previous speculation hypothesis. Furthermore, the contribution of marine sources was greater to TMDEAH^+ than to DMAH^+ in all campaigns, which corresponded to the higher ratio of $\text{TMDEAH}^+/\text{DMAH}^+$ in the samples influenced primarily by marine air masses (Fig. 4312). It should be pointed out that although aminium/ NH_4^+ ratios could vary with the chemistry of aerosols due to slightly different gas-to-particle partitioning of the amines and NH_3 (Chan and Chan, 2013; Pankow, 2015; Xie et al., 2018) and marine aminiums may also partially originated from primary source as discussed above. Therefore, our discussion is constrained on the source analysis of aerosol aminiums, but not gaseous or total amines (gaseous amines + aerosol aminiums). Although NH_4^+ was mainly derived from the land, marine sources may also had a certain contribution (Altieri et al., 2014; Paulot et al., 2015). This was neglected in our calculation and might lead to the overestimate of terrestrial contributions to aminiums. Besides, the relatively small number of data points used in the fitting (25 points) and the treatment of $([\text{aminium}]/[\text{NH}_4^+])_{\text{terrestrial}}$ as a fixed value ignoring its variation would cause uncertainty in the results. Nonetheless, this our method is the first quantitative estimate of attempt to calculate the contributions of marine biogenic and terrestrial and marine sources to aerosol aminiums over the coastal ECS sea, which will provide an insight of sources and roles of amines in the atmosphere, and the method using $\text{MSA}/\text{nss-SO}_4^{2-}$ as an indicator of marine source is rational and feasible.

4 Conclusion

Amines in the atmosphere play an important role in new particle formation and subsequent particle growth, and studying aerosol aminiums can provide insight into the sources, reaction pathways and environmental effects of amines. An integrated observation was conducted on aerosol aminiums ~~mainly~~ (DMAH⁺, TMDEAH⁺ and TEAH⁺) in a coastal city (Shanghai), a nearby island (Huaniao) and the marginal seas (the YECS). All three aminiums exhibited ~~significantly~~ significant seasonal variation in Shanghai with their highest concentrations in winter, which was consistent with relatively severe air pollution associated with the winter monsoon (continental winds) and the lowest BLH and temperature in this season. Atmospheric oxidizing capacity and relative humidity may also influence the concentrations of aerosol aminiums to some extent by oxidizing gaseous amines and enhancing the gas-particle partitioning, respectively. By comparing the ocean sites to Shanghai, similar concentrations of DMAH⁺ and 3-fold higher TMDEAH⁺ were observed suggesting that these two aminiums may have significant marine sources. ~~Differently~~ By contrast, TEAH⁺ was ~~most~~ abundant aminium in Shanghai but it was below the detection limit over Huaniao Island and the YECS, implying its terrestrial origin.

Aminiums influenced substantially by terrestrial transport showed a bimodal distribution with two peaks at 0.18–0.32 μm (condensation mode) and 0.56–1.0 μm (droplet mode), suggesting that the gas-to-particle condensation and cloud processing were ~~primary~~ main formation pathways for aerosol aminiums. Nonetheless, aminiums demonstrated a unimodal distribution with a wide peak at 0.18–1.0 μm over the YECS and in late summer of Huaniao Island, and the elevated concentration at 0.32–0.56 μm might be related to sea-spray aerosols that either contain primary aminiums or provide surface for heterogeneous reactions to form secondary aminiums. This indicates that aminiums in marine aerosols may undergo different formation pathways from those on ~~the~~ land.

We ~~firstly~~ distinguished the contributions of terrestrial and marine sources to aerosol aminiums for the first time by taking the mass ratio of MSA to nss-SO_4^{2-} as an indicator of marine biogenic sources. In the autumn of 2016, the contributions of terrestrial sources to aminiums over Huaniao Island were estimated to be more than 60%. ~~In~~ By contrast, marine biogenic sources dominated aminium concentrations especially for TMDEAH⁺ (~80%) in the summer of 2017. ~~The proposed quantitative estimates may be helpful for simulating the source emissions of amines in atmospheric chemistry models in the coastal area.~~ Our results indicated that marine biogenic emission of amines could not be ignored in the eastern coast of China, especially in summer. Therefore, it is necessary to add this source into the emission inventory of amines and recent modelling of amines over eastern China without marine source (Mao et al., 2018) may result in significant deviations. Besides, the role of amines in new particle formation over the open ocean is likely to be more important due to much less pollutants \compared to the coastal area, which should be further studied.

Data availability: Data are available from the corresponding author on request (yingchen@fudan.edu.cn).

Author contribution. SZ, YC and CD conceived the study. SZ, YC and CD wrote the paper. SZ, HL, and JX collected the samples. SZ, TY and JX performed the measurement. All have contributed to review of the manuscript.

Competing interests. The authors declare that they have no conflict of interest.

Acknowledgements. This work is jointly supported by the National Key Research and Development Program of China (2016YFA0601304), National Natural Science Foundation of China (41775145) and Fudan's Undergraduate Research Opportunities Program (15100). We gratefully acknowledge the NOAA Air Resources Laboratory (ARL) for the provision of the HYSPLIT model used in this publication and the National Climatic Data Center (NCDC) for the archived observed surface meteorological data. The MODIS chlorophyll a data was downloaded from NASA OceanColor website

(<https://oceancolor.gsfc.nasa.gov/>). We are sincerely grateful to Huaniao Lighthouse maintained by Shanghai Maritime Safety Administration for providing the long-term sampling site and fisherman Yueping Chen and his wife for sampling assistance at Huaniao Island. We also thank all of the sailors onboard R/V *Dongfanghong II* for their logistical support during the cruise. Shengqian Zhou sincerely acknowledge Bo Wang, Xiaofei Qin, Tianfeng Guo, Fanghui Wang and Yucheng Zhu for their assistance with field and laboratory work.

References

- Almeida, J., Schobesberger, S., Kurten, A., Ortega, I. K., Kupiainen-Maatta, O., Praplan, A. P., Adamov, A., Amorim, A., Bianchi, F., Breitenlechner, M., David, A., Dommen, J., Donahue, N. M., Downard, A., Dunne, E., Duplissy, J., Ehrhart, S., Flagan, R. C., Franchin, A., Guida, R., Hakala, J., Hansel, A., Heinritzi, M., Henschel, H., Jokinen, T., Junninen, H., Kajos, M., Kangasluoma, J., Keskinen, H., Kupe, A., Kurten, T., Kvashin, A. N., Laaksonen, A., Lehtipalo, K., Leiminger, M., Leppa, J., Loukonen, V., Makhmutov, V., Mathot, S., McGrath, M. J., Nieminen, T., Olenius, T., Onnela, A., Petaja, T., Riccobono, F., Riipinen, I., Rissanen, M., Rondo, L., Ruuskanen, T., Santos, F. D., Sarnela, N., Schallhart, S., Schnitzhofer, R., Seinfeld, J. H., Simon, M., Sipila, M., Stozhkov, Y., Stratmann, F., Tome, A., Trostl, J., Tsagkogeorgas, G., Vaattovaara, P., Viisanen, Y., Virtanen, A., Vrtala, A., Wagner, P. E., Weingartner, E., Wex, H., Williamson, C., Wimmer, D., Ye, P., Yli-Juuti, T., Carslaw, K. S., Kulmala, M., Curtius, J., Baltensperger, U., Worsnop, D. R., Vehkamäki, H., and Kirkby, J.: Molecular understanding of sulphuric acid-amine particle nucleation in the atmosphere, *Nature*, 502, 359-363, <https://doi.org/10.1038/nature12663>, 2013.
- Altieri, K. E., Hastings, M. G., Peters, A. J., Oleynik, S., and Sigman, D. M.: Isotopic evidence for a marine ammonium source in rainwater at Bermuda, *Global Biogeochem. Cy.*, 28, 1066-1080, <https://doi.org/10.1002/2014GB004809>, 2014.
- Barnes, I., Hjorth, J., and Mihalopoulos, N.: Dimethyl sulfide and dimethyl sulfoxide and their oxidation in the atmosphere, *Chem. Rev.*, 106, 940-975, <https://doi.org/10.1021/cr020529+>, 2006.
- [Bates, T. S., Quinn, P. K., Frossard, A. A., Russell, L. M., Hakala, J., Petäjä, T., Kulmala, M., Covert, D. S., Cappa, C. D., Li, S. M., Hayden, K. L., Nuaaman, I., McLaren, R., Massoli, P., Canagaratna, M. R., Onasch, T. B., Sueper, D., Worsnop, D. R., and Keene, W. C.: Measurements of ocean derived aerosol off the coast of California, *J. Geophys. Res.-Atmos.*, 117, n/a-n/a, <https://doi.org/10.1029/2012jd017588>, 2012.](#)
- Bian, Q., Huang, X. H. H., and Yu, J. Z.: One-year observations of size distribution characteristics of major aerosol constituents at a coastal receptor site in Hong Kong – Part 1: Inorganic ions and oxalate, *Atmos. Chem. Phys.*, 14, 9013-9027, <https://doi.org/10.5194/acp-14-9013-2014>, 2014.
- Calderón, S. M., Poor, N. D., and Campbell, S. W.: Estimation of the particle and gas scavenging contributions to wet deposition of organic nitrogen, *Atmos. Environ.*, 41, 4281-4290, <https://doi.org/10.1016/j.atmosenv.2006.06.067>, 2007.
- Chan, L. P., and Chan, C. K.: Role of the aerosol phase state in ammonia/amines exchange reactions, *Environ. Sci. Technol.*, 47, 5755-5762, <https://doi.org/10.1021/es4004685>, 2013.
- Charlson, R. J., Lovelock, J. E., Andreae, M. O., and Warren, S. G.: Oceanic phytoplankton, atmospheric sulphur, cloud albedo and climate, *Nature*, 326, 655-661, <https://doi.org/10.1038/326655a0>, 1987.
- [Dall'Osto, M., Airs, R., Beale, R., Cree, C., Fitzsimons, M., Beddows, D. C. S., Harrison, R. M., Ceburnis, D., O'Dowd, C., Rinaldi, M., Paglione, M., Nenes, A., Decesari, S., and Simo, R.: Simultaneous detection of alkylamines in the surface ocean and atmosphere of the Antarctic sympagic environment, *ACS Earth Space Chem.*, <https://doi.org/10.1021/acsearthspacechem.9b00028>, 2019.](#)
- [Dawson, M. L., Perraud, V., Gomez, A., Arquero, K. D., Ezell, M. J., and Finlayson-Pitts, B. J.: Measurement of gas-phase ammonia and amines in air by collection onto an ion exchange resin and analysis by ion chromatography, *Atmos. Meas. Tech.*, 7, 2733-2744, <https://doi.org/10.5194/amt-7-2733-2014>, 2014.](#)

Erupe, M. E., Viggiano, A. A., and Lee, S. H.: The effect of trimethylamine on atmospheric nucleation involving H₂SO₄, *Atmos. Chem. Phys.*, 11, 4767-4775, <https://doi.org/10.5194/acp-11-4767-2011>, 2011.

Facchini, M. C., Decesari, S., Rinaldi, M., Carbone, C., Finessi, E., Mircea, M., Fuzzi, S., Moretti, F., Tagliavini, E., Ceburnis, D., and O'Dowd, C. D.: Important source of marine secondary organic aerosol from biogenic amines, *Environ. Sci. Technol.*, 42, 9116-9121, <https://doi.org/10.1021/es8018385>, 2008.

Faloon, I.: Sulfur processing in the marine atmospheric boundary layer: A review and critical assessment of modeling uncertainties, *Atmos. Environ.*, 43, 2841-2854, <https://doi.org/10.1016/j.atmosenv.2009.02.043>, 2009.

Frossard, A. A., Russell, L. M., Burrows, S. M., Elliott, S. M., Bates, T. S., and Quinn, P. K.: Sources and composition of submicron organic mass in marine aerosol particles, *J. Geophys. Res.-Atmos.*, 119, 12,977-913,003, <https://doi.org/10.1002/2014jd021913>, 2014.

Ge, X., Wexler, A. S., and Clegg, S. L.: Atmospheric amines – Part II. Thermodynamic properties and gas/particle partitioning, *Atmos. Environ.*, 45, 561-577, <https://doi.org/10.1016/j.atmosenv.2010.10.013>, 2011a.

Ge, X., Wexler, A. S., and Clegg, S. L.: Atmospheric amines – Part I. A review, *Atmos. Environ.*, 45, 524-546, <https://doi.org/10.1016/j.atmosenv.2010.10.012>, 2011b.

Gibb, S. W., Mantoura, R. F. C., and Liss, P. S.: Ocean-atmosphere exchange and atmospheric speciation of ammonia and methylamines in the region of the NW Arabian Sea, *Global Biogeochem. Cy.*, 13, 161-178, <https://doi.org/10.1029/98gb00743>, 1999.

Hemmilä, M., Hellén, H., Virkkula, A., Makkonen, U., Praplan, A. P., Kontkanen, J., Ahonen, L., Kulmala, M., and Hakola, H.: Amines in boreal forest air at SMEAR II station in Finland, *Atmos. Chem. Phys.*, 18, 6367-6380, <https://doi.org/10.5194/acp-18-6367-2018>, 2018.

Ho, K. F., Ho, S. S. H., Huang, R.-J., Liu, S. X., Cao, J.-J., Zhang, T., Chuang, H.-C., Chan, C. S., Hu, D., and Tian, L.: Characteristics of water-soluble organic nitrogen in fine particulate matter in the continental area of China, *Atmos. Environ.*, 106, 252-261, <https://doi.org/10.1016/j.atmosenv.2015.02.010>, 2015.

Hu, Q., Yu, P., Zhu, Y., Li, K., Gao, H., and Yao, X.: Concentration, Size Distribution, and Formation of Trimethylaminium and Dimethylaminium Ions in Atmospheric Particles over Marginal Seas of China, *J. Atmos. Sci.*, 72, 3487-3498, <https://doi.org/10.1175/jas-d-14-0393.1>, 2015.

Hu, Q., Qu, K., Gao, H., Cui, Z., Gao, Y., and Yao, X.: Large increases in primary trimethylaminium and secondary dimethylaminium in atmospheric particles associated with cyclonic eddies in the northwest Pacific Ocean, *J. Geophys. Res.-Atmos.*, <https://doi.org/10.1029/2018jd028836>, 2018.

Huang, R. J., Li, W. B., Wang, Y. R., Wang, Q. Y., Jia, W. T., Ho, K. F., Cao, J. J., Wang, G. H., Chen, X., El Haddad, I., Zhuang, Z. X., Wang, X. R., Prévôt, A. S. H., O'Dowd, C. D., and Hoffmann, T.: Determination of alkylamines in atmospheric aerosol particles: a comparison of gas chromatography–mass spectrometry and ion chromatography approaches, *Atmos. Meas. Tech.*, 7, 2027-2035, <https://doi.org/10.5194/amt-7-2027-2014>, 2014.

Huang, X., Deng, C., Zhuang, G., Lin, J., and Xiao, M.: Quantitative analysis of aliphatic amines in urban aerosols based on online derivatization and high performance liquid chromatography, *Environ. Sci.-Proc. Imp.*, 18, 796-801, <https://doi.org/10.1039/c6em00197a>, 2016.

Huang, Y., Chen, H., Wang, L., Yang, X., and Chen, J.: Single particle analysis of amines in ambient aerosol in Shanghai, *Environ. Chem.*, 9, 202, <https://doi.org/10.1071/en11145>, 2012.

Kupiainen, O., Ortega, I. K., Kurten, T., and Vehkamäki, H.: Amine substitution into sulfuric acid - ammonia clusters, *Atmos. Chem. Phys.*, 12, 3591-3599, <https://doi.org/10.5194/acp-12-3591-2012>, 2012.

Kurten, A., Jokinen, T., Simon, M., Sipilä, M., Sarnela, N., Junninen, H., Adamov, A., Almeida, J., Amorim, A., Bianchi, F., Breitenlechner, M., Dommen, J., Donahue, N. M., Duplissy, J., Ehrhart, S., Flagan, R. C., Franchin, A., Hakala, J., Hansel, A., Heinritzi, M., Hutterli, M., Kangasluoma, J., Kirkby, J., Laaksonen, A., Lehtipalo, K., Leiminger, M., Makhmutov, V., Mathot,

S., Onnela, A., Petaja, T., Praplan, A. P., Riccobono, F., Rissanen, M. P., Rondo, L., Schobesberger, S., Seinfeld, J. H., Steiner, G., Tome, A., Trostl, J., Winkler, P. M., Williamson, C., Wimmer, D., Ye, P., Baltensperger, U., Carslaw, K. S., Kulmala, M., Worsnop, D. R., and Curtius, J.: Neutral molecular cluster formation of sulfuric acid-dimethylamine observed in real time under atmospheric conditions, *P. Natl. Acad. Sci. USA*, 111, 15019-15024, <https://doi.org/10.1073/pnas.1404853111>, 2014.

Kürten, A., Bergen, A., Heinritzi, M., Leiminger, M., Lorenz, V., Piel, F., Simon, M., Sitals, R., Wagner, A. C., and Curtius, J.: Observation of new particle formation and measurement of sulfuric acid, ammonia, amines and highly oxidized organic molecules at a rural site in central Germany, *Atmos. Chem. Phys.*, 16, 12793-12813, <https://doi.org/10.5194/acp-16-12793-2016>, 2016.

Kurten, T., Loukonen, V., Vehkamäki, H., and Kulmala, M.: Amines are likely to enhance neutral and ion-induced sulfuric acid-water nucleation in the atmosphere more effectively than ammonia, *Atmos. Chem. Phys.*, 8, 4095-4103, <https://doi.org/10.5194/acp-8-4095-2008>, 2008.

Liu, F., Bi, X., Zhang, G., Peng, L., Lian, X., Lu, H., Fu, Y., Wang, X., Peng, P. a., and Sheng, G.: Concentration, size distribution and dry deposition of amines in atmospheric particles of urban Guangzhou, China, *Atmos. Environ.*, 171, 279-288, <https://doi.org/10.1016/j.atmosenv.2017.10.016>, 2017.

Liu, F., Bi, X., Zhang, G., Lian, X., Fu, Y., Yang, Y., Lin, Q., Jiang, F., Wang, X., Peng, P. a., and Sheng, G.: Gas-to-particle partitioning of atmospheric amines observed at a mountain site in southern China, *Atmos. Environ.*, 195, 1-11, <https://doi.org/10.1016/j.atmosenv.2018.09.038>, 2018a.

Liu, X.-H., Zhang, Y., Cheng, S.-H., Xing, J., Zhang, Q., Streets, D. G., Jang, C., Wang, W.-X., and Hao, J.-M.: Understanding of regional air pollution over China using CMAQ, part I performance evaluation and seasonal variation, *Atmos. Environ.*, 44, 2415-2426, <https://doi.org/10.1016/j.atmosenv.2010.03.035>, 2010.

Liu, X., Li, J., Qu, Y., Han, T., Hou, L., Gu, J., Chen, C., Yang, Y., Liu, X., and Yang, T.: Formation and evolution mechanism of regional haze: a case study in the megacity Beijing, China, *Atmos. Chem. Phys.*, 13, 4501-4514, <https://doi.org/10.5194/acp-13-4501-2013>, 2013.

Liu, Y., Han, C., Liu, C., Ma, J., Ma, Q., and He, H.: Differences in the reactivity of ammonium salts with methylamine, *Atmos. Chem. Phys.*, 12, 4855-4865, <https://doi.org/10.5194/acp-12-4855-2012>, 2012.

Liu, Y., Fan, Q., Chen, X., Zhao, J., Ling, Z., Hong, Y., Li, W., Chen, X., Wang, M., and Wei, X.: Modeling the impact of chlorine emissions from coal combustion and prescribed waste incineration on tropospheric ozone formation in China, *Atmos. Chem. Phys.*, 18, 2709-2724, <https://doi.org/10.5194/acp-18-2709-2018>, 2018b.

Logan, J. A.: Tropospheric ozone: Seasonal behavior, trends, and anthropogenic influence, *J. Geophys. Res.-Atmos.*, 90, 10463-10482, <https://doi.org/10.1029/JD090iD06p10463>, 1985.

Loukonen, V., Kurtén, T., Ortega, I. K., Vehkamäki, H., Pádua, A. A. H., Sellegri, K., and Kulmala, M.: Enhancing effect of dimethylamine in sulfuric acid nucleation in the presence of water – a computational study, *Atmos. Chem. Phys.*, 10, 4961-4974, <https://doi.org/10.5194/acp-10-4961-2010>, 2010.

Mao, J., Yu, F., Zhang, Y., An, J., Wang, L., Zheng, J., Yao, L., Luo, G., Ma, W., Yu, Q., Huang, C., Li, L., and Chen, L.: High-resolution modeling of gaseous methylamines over a polluted region in China: source-dependent emissions and implications of spatial variations, *Atmos. Chem. Phys.*, 18, 7933-7950, <https://doi.org/10.5194/acp-18-7933-2018>, 2018.

Müller, C., Iinuma, Y., Karstensen, J., van Pinxteren, D., Lehmann, S., Gnauk, T., and Herrmann, H.: Seasonal variation of aliphatic amines in marine sub-micrometer particles at the Cape Verde islands, *Atmos. Chem. Phys.*, 9, 9587-9597, <https://doi.org/10.5194/acp-9-9587-2009>, 2009.

Murphy, S. M., Sorooshian, A., Kroll, J. H., Ng, N. L., Chhabra, P., Tong, C., Surratt, J. D., Knipping, E., Flagan, R. C., and Seinfeld, J. H.: Secondary aerosol formation from atmospheric reactions of aliphatic amines, *Atmos. Chem. Phys.*, 7, 2313-2337, <https://doi.org/10.5194/acp-7-2313-2007>, 2007.

Nielsen, C. J., Herrmann, H., and Weller, C.: Atmospheric chemistry and environmental impact of the use of amines in carbon

capture and storage (CCS), *Chem. Soc. Rev.*, 41, 6684-6704, <https://doi.org/10.1039/c2cs35059a>, 2012.

Olenius, T., Halonen, R., Kurtén, T., Henschel, H., Kupiainen-Määttä, O., Ortega, I. K., Jen, C. N., Vehkamäki, H., and Riipinen, I.: New particle formation from sulfuric acid and amines: Comparison of monomethylamine, dimethylamine, and trimethylamine, *J. Geophys. Res.-Atmos.*, 122, 7103-7118, <https://doi.org/10.1002/2017jd026501>, 2017.

Paasonen, P., Olenius, T., Kupiainen, O., Kurten, T., Petaja, T., Birmili, W., Hamed, A., Hu, M., Huey, L. G., Plass-Duelmer, C., Smith, J. N., Wiedensohler, A., Loukonen, V., McGrath, M. J., Ortega, I. K., Laaksonen, A., Vehkamäki, H., Kerminen, V. M., and Kulmala, M.: On the formation of sulphuric acid - amine clusters in varying atmospheric conditions and its influence on atmospheric new particle formation, *Atmos. Chem. Phys.*, 12, 9113-9133, <https://doi.org/10.5194/acp-12-9113-2012>, 2012.

Pankow, J. F.: Phase considerations in the gas/particle partitioning of organic amines in the atmosphere, *Atmos. Environ.*, 122, 448-453, <https://doi.org/10.1016/j.atmosenv.2015.09.056>, 2015.

Paulot, F., Jacob, D. J., Johnson, M. T., Bell, T. G., Baker, A. R., Keene, W. C., Lima, I. D., Doney, S. C., and Stock, C. A.: Global oceanic emission of ammonia: Constraints from seawater and atmospheric observations, *Global Biogeochem. Cy.*, 29, 1165-1178, <https://doi.org/10.1002/2015gb005106>, 2015.

Perrone, M. G., Zhou, J., Malandrino, M., Sangiorgi, G., Rizzi, C., Ferrero, L., Dommen, J., and Bolzacchini, E.: PM chemical composition and oxidative potential of the soluble fraction of particles at two sites in the urban area of Milan, Northern Italy, *Atmos. Environ.*, 128, 104-113, <https://doi.org/10.1016/j.atmosenv.2015.12.040>, 2016.

Rehbein, P. J., Jeong, C. H., McGuire, M. L., Yao, X., Corbin, J. C., and Evans, G. J.: Cloud and fog processing enhanced gas-to-particle partitioning of trimethylamine, *Environ. Sci. Technol.*, 45, 4346-4352, <https://doi.org/10.1021/es1042113>, 2011.

Rinaldi, M., Decesari, S., Finessi, E., Giulianelli, L., Carbone, C., Fuzzi, S., O'Dowd, C. D., Ceburnis, D., and Facchini, M. C.: Primary and Secondary Organic Marine Aerosol and Oceanic Biological Activity: Recent Results and New Perspectives for Future Studies, *Adv. Meteorol.*, 2010, 1-10, <https://doi.org/10.1155/2010/310682>, 2010.

Saltzman, E., Savoie, D., Prospero, J., and Zika, R.: Atmospheric methanesulfonic acid and non - sea - salt sulfate at Fanning and American Samoa, *Geophys. Res. Lett.*, 12, 437-440, <https://doi.org/10.1029/GL012i007p00437>, 1985.

Shen, W., Ren, L., Zhao, Y., Zhou, L., Dai, L., Ge, X., Kong, S., Yan, Q., Xu, H., Jiang, Y., He, J., Chen, M., and Yu, H.: C1-C2 alkyl aminiums in urban aerosols: Insights from ambient and fuel combustion emission measurements in the Yangtze River Delta region of China, *Environ. Pollut.*, 230, 12-21, <https://doi.org/10.1016/j.envpol.2017.06.034>, 2017.

Smith, J. N., Barsanti, K. C., Friedli, H. R., Ehn, M., Kulmala, M., Collins, D. R., Scheckman, J. H., Williams, B. J., and McMurry, P. H.: Observations of aminium salts in atmospheric nanoparticles and possible climatic implications, *P. Natl. Acad. Sci. USA*, 107, 6634-6639, <https://doi.org/10.1073/pnas.0912127107>, 2010.

Sorooshian, A., Padró, L. T., Nenes, A., Feingold, G., McComiskey, A., Hersey, S. P., Gates, H., Jonsson, H. H., Miller, S. D., Stephens, G. L., Flagan, R. C., and Seinfeld, J. H.: On the link between ocean biota emissions, aerosol, and maritime clouds: Airborne, ground, and satellite measurements off the coast of California, *Global Biogeochem. Cy.*, 23, n/a-n/a, <https://doi.org/10.1029/2009gb003464>, 2009.

Souza, S.: Low molecular weight carboxylic acids in an urban atmosphere: Winter measurements in São Paulo City, Brazil, *Atmos. Environ.*, 33, 2563-2574, [https://doi.org/10.1016/s1352-2310\(98\)00383-5](https://doi.org/10.1016/s1352-2310(98)00383-5), 1999.

Tang, X., Price, D., Praske, E., Vu, D. N., Purvis-Roberts, K., Silva, P. J., Cocker III, D. R., and Asa-Awuku, A.: Cloud condensation nuclei (CCN) activity of aliphatic amine secondary aerosol, *Atmos. Chem. Phys.*, 14, 5959-5967, <https://doi.org/10.5194/acp-14-5959-2014>, 2014.

Tao, Y., Ye, X., Jiang, S., Yang, X., Chen, J., Xie, Y., and Wang, R.: Effects of amines on particle growth observed in new particle formation events, *J. Geophys. Res.-Atmos.*, 121, 324-335, <https://doi.org/10.1002/2015jd024245>, 2016.

Tao, Y., and Murphy, J. G.: Evidence for the importance of semi-volatile organic ammonium salts in ambient particulate matter, *Environ. Sci. Technol.*, 53, 108-116, <https://doi.org/10.1021/acs.est.8b03800>, 2018.

Thompson, A. M.: The oxidizing capacity of the Earth's atmosphere: Probable past and future changes, *Science*, 256, 1157-

1165, <https://doi.org/10.1126/science.256.5060.1157>, 1992.

Tian, H. Z., Zhu, C. Y., Gao, J. J., Cheng, K., Hao, J. M., Wang, K., Hua, S. B., Wang, Y., and Zhou, J. R.: Quantitative assessment of atmospheric emissions of toxic heavy metals from anthropogenic sources in China: historical trend, spatial distribution, uncertainties, and control policies, *Atmos. Chem. Phys.*, 15, 10127-10147, <https://doi.org/10.5194/acp-15-10127-2015>, 2015.

~~Tsai, Y. I., Sopajaree, K., Chotruksa, A., Wu, H. C., and Kuo, S. C.: Source indicators of biomass burning associated with inorganic salts and carboxylates in dry-season ambient aerosol in Chiang Mai Basin, Thailand, *Atmos. Environ.*, 78, 93-104, <https://doi.org/10.1016/j.atmosenv.2012.09.040>, 2013.~~

Uno, I., Osada, K., Yumimoto, K., Wang, Z., Itahashi, S., Pan, X., Hara, Y., Kanaya, Y., Yamamoto, S., and Fairlie, T. D.: Seasonal variation of fine- and coarse-mode nitrates and related aerosols over East Asia: synergetic observations and chemical transport model analysis, *Atmos. Chem. Phys.*, 17, 14181-14197, <https://doi.org/10.5194/acp-17-14181-2017>, 2017.

VandenBoer, T. C., Petroff, A., Markovic, M. Z., and Murphy, J. G.: Size distribution of alkyl amines in continental particulate matter and their online detection in the gas and particle phase, *Atmos. Chem. Phys.*, 11, 4319-4332, <https://doi.org/10.5194/acp-11-4319-2011>, 2011.

VandenBoer, T. C., Markovic, M. Z., Petroff, A., Czar, M. F., Borduas, N., and Murphy, J. G.: Ion chromatographic separation and quantitation of alkyl methylamines and ethylamines in atmospheric gas and particulate matter using preconcentration and suppressed conductivity detection, *J. Chromatogr. A*, 1252, 74-83, <https://doi.org/10.1016/j.chroma.2012.06.062>, 2012.

Violaki, K., and Mihalopoulos, N.: Water-soluble organic nitrogen (WSON) in size-segregated atmospheric particles over the Eastern Mediterranean, *Atmos. Environ.*, 44, 4339-4345, <https://doi.org/10.1016/j.atmosenv.2010.07.056>, 2010.

Wang, B., Chen, Y., Zhou, S., Li, H., Wang, F., and Yang, T.: The influence of terrestrial transport on visibility and aerosol properties over the coastal East China Sea, *Sci. Total. Environ.*, 649, 652-660, <https://doi.org/10.1016/j.scitotenv.2018.08.312>, 2018.

Wang, F., Chen, Y., Meng, X., Fu, J., and Wang, B.: The contribution of anthropogenic sources to the aerosols over East China Sea, *Atmos. Environ.*, 127, 22-33, <https://doi.org/10.1016/j.atmosenv.2015.12.002>, 2016.

Wang, L., Khalizov, A. F., Zheng, J., Xu, W., Ma, Y., Lal, V., and Zhang, R.: Atmospheric nanoparticles formed from heterogeneous reactions of organics, *Nat. Geosci.*, 3, 238-242, <https://doi.org/10.1038/ngeo778>, 2010a.

Wang, L., Lal, V., Khalizov, A. F., and Zhang, R.: Heterogeneous chemistry of alkylamines with sulfuric acid: implications for atmospheric formation of alkylammonium sulfates, *Environ. Sci. Technol.*, 44, 2461-2465, <https://doi.org/10.1021/es9036868>, 2010b.

Xie, H., Feng, L., Hu, Q., Zhu, Y., Gao, H., Gao, Y., and Yao, X.: Concentration and size distribution of water-extracted dimethylammonium and trimethylammonium in atmospheric particles during nine campaigns - Implications for sources, phase states and formation pathways, *Sci. Total. Environ.*, 631-632, 130-141, <https://doi.org/10.1016/j.scitotenv.2018.02.303>, 2018.

Yang, G.-P., Zhang, H.-H., Su, L.-P., and Zhou, L.-M.: Biogenic emission of dimethylsulfide (DMS) from the North Yellow Sea, China and its contribution to sulfate in aerosol during summer, *Atmos. Environ.*, 43, 2196-2203, <https://doi.org/10.1016/j.atmosenv.2009.01.011>, 2009.

Yang, G.-P., Zhang, S.-H., Zhang, H.-H., Yang, J., and Liu, C.-Y.: Distribution of biogenic sulfur in the Bohai Sea and northern Yellow Sea and its contribution to atmospheric sulfate aerosol in the late fall, *Mar. Chem.*, 169, 23-32, <https://doi.org/10.1016/j.marchem.2014.12.008>, 2015.

Yao, L., Wang, M.-Y., Wang, X.-K., Liu, Y.-J., Chen, H.-F., Zheng, J., Nie, W., Ding, A.-J., Geng, F.-H., Wang, D.-F., Chen, J.-M., Worsnop, D. R., and Wang, L.: Detection of atmospheric gaseous amines and amides by a high-resolution time-of-flight chemical ionization mass spectrometer with protonated ethanol reagent ions, *Atmos. Chem. Phys.*, 16, 14527-14543, <https://doi.org/10.5194/acp-16-14527-2016>, 2016.

Yao, L., Garmash, O., Bianchi, F., Zheng, J., Yan, C., Kontkanen, J., Junninen, H., Mazon, S. B., Ehn, M., Paasonen, P., Sipila,

663 M., Wang, M., Wang, X., Xiao, S., Chen, H., Lu, Y., Zhang, B., Wang, D., Fu, Q., Geng, F., Li, L., Wang, H., Qiao, L., Yang,
664 X., Chen, J., Kerminen, V. M., Petaja, T., Worsnop, D. R., Kulmala, M., and Wang, L.: Atmospheric new particle formation
665 from sulfuric acid and amines in a Chinese megacity, *Science*, 361, 278-281, <https://doi.org/10.1126/science.aao4839>, 2018.

666 [You, Y., Kanawade, V. P., de Gouw, J. A., Guenther, A. B., Madronich, S., Sierra-Hernández, M. R., Lawler, M., Smith, J. N.,](#)
667 [Takahama, S., Ruggeri, G., Koss, A., Olson, K., Baumann, K., Weber, R. J., Nenes, A., Guo, H., Edgerton, E. S., Porcelli, L.,](#)
668 [Brune, W. H., Goldstein, A. H., and Lee, S. H.: Atmospheric amines and ammonia measured with a chemical ionization mass](#)
669 [spectrometer \(CIMS\), *Atmos. Chem. Phys.*, 14, 12181-12194, <https://doi.org/10.5194/acp-14-12181-2014>, 2014.](#)

670 Yu, F., and Luo, G.: Modeling of gaseous methylamines in the global atmosphere: impacts of oxidation and aerosol uptake,
671 *Atmos. Chem. Phys.*, 14, 12455-12464, <https://doi.org/10.5194/acp-14-12455-2014>, 2014.

672 Yu, H., McGraw, R., and Lee, S.-H.: Effects of amines on formation of sub-3 nm particles and their subsequent growth,
673 *Geophys. Res. Lett.*, 39, n/a-n/a, <https://doi.org/10.1029/2011gl050099>, 2012.

674 Yu, P., Hu, Q., Li, K., Zhu, Y., Liu, X., Gao, H., and Yao, X.: Characteristics of dimethylammonium and trimethylammonium in
675 atmospheric particles ranging from supermicron to nanometer sizes over eutrophic marginal seas of China and oligotrophic
676 open oceans, *Sci. Total. Environ.*, 572, 813-824, <https://doi.org/10.1016/j.scitotenv.2016.07.114>, 2016.

677 Yuan, H., Wang, Y., and Zhuang, G.: MSA in Beijing aerosol, *Chinese Sci. Bull.*, 49, 1020, 10.1360/03wb0186, 2004.

678 Zhang, G., Bi, X., Chan, L. Y., Li, L., Wang, X., Feng, J., Sheng, G., Fu, J., Li, M., and Zhou, Z.: Enhanced trimethylamine-
679 containing particles during fog events detected by single particle aerosol mass spectrometry in urban Guangzhou, China, *Atmos.*
680 *Environ.*, 55, 121-126, <https://doi.org/10.1016/j.atmosenv.2012.03.038>, 2012.

681 Zheng, J., Ma, Y., Chen, M., Zhang, Q., Wang, L., Khalizov, A. F., Yao, L., Wang, Z., Wang, X., and Chen, L.: Measurement
682 of atmospheric amines and ammonia using the high resolution time-of-flight chemical ionization mass spectrometry, *Atmos.*
683 *Environ.*, 102, 249-259, <https://doi.org/10.1016/j.atmosenv.2014.12.002>, 2015.

684 Zhou, S., Lin, J., Qin, X., Chen, Y., and Deng, C.: Determination of atmospheric alkylamines by ion chromatography using
685 18-crown-6 as mobile phase additive, *J Chromatogr. A*, 1563, 154-161, <https://doi.org/10.1016/j.chroma.2018.05.074>, 2018.

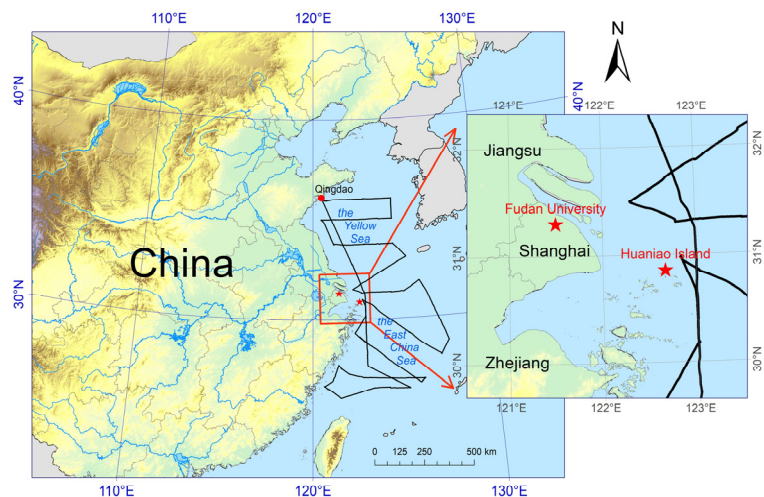


Figure 1. Map of sampling sites and area. The red stars represent the locations of Shanghai (Fudan University) and Huaniao Island, and the black line in the marginal seas represents the cruise track in the spring of 2017.

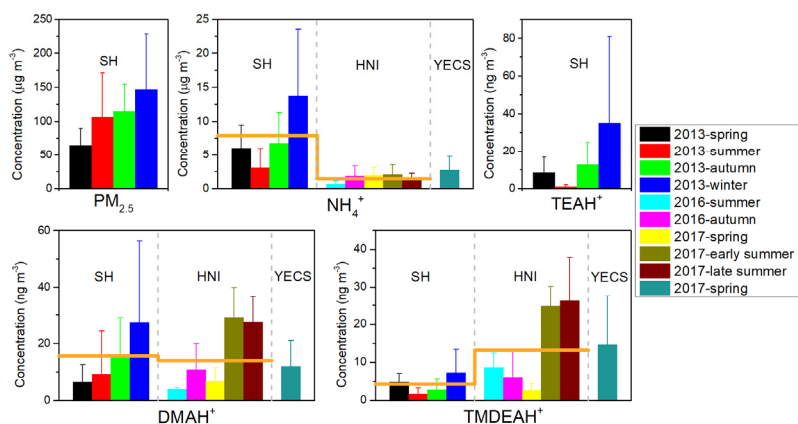


Figure 2. The mass concentrations of PM_{2.5}, fine-particle NH₄⁺ and three aminiums (TEAH⁺, DMAH⁺ and TMDEAH⁺) in different campaigns in Shanghai (SH), Huaniao Island (HNI) and the Yellow and East China seas (YECS). The columns and error bars represent average concentrations and standard deviations, respectively. The orange horizontal lines represent the annual average concentrations of aminiums in SH and HNI.

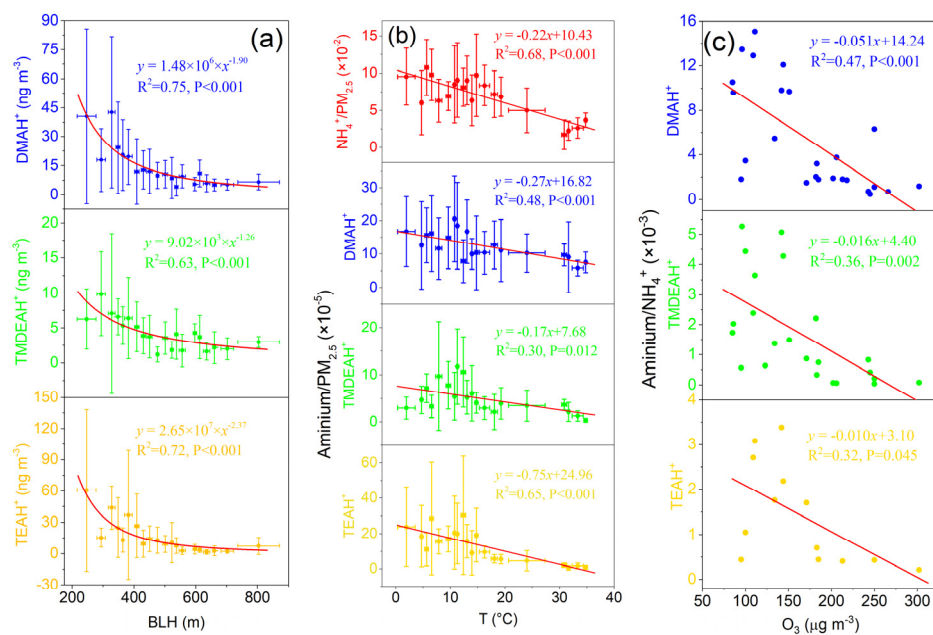
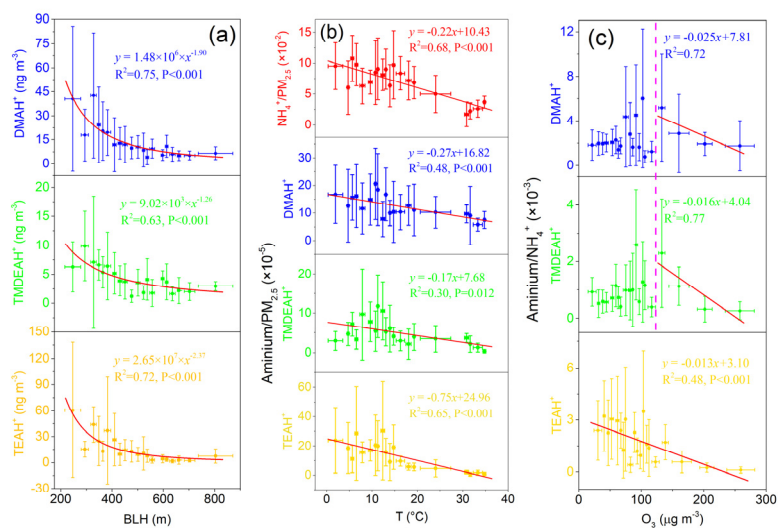


Figure 3. (a) Relationships between concentrations of aminiums and boundary layer height (BLH) over Shanghai in 2013. (b) Relationships between mass ratios of aminiums and NH_4^+ to $\text{PM}_{2.5}$ and temperature over Shanghai in 2013. (c) Relationships between mass ratios of aminiums to NH_4^+ and O_3 concentrations over Shanghai during the summer of 2013.

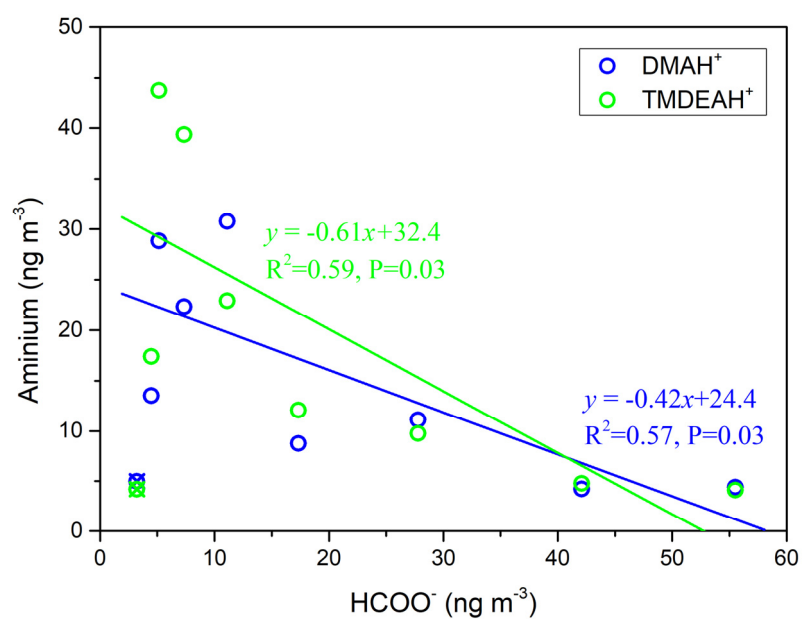
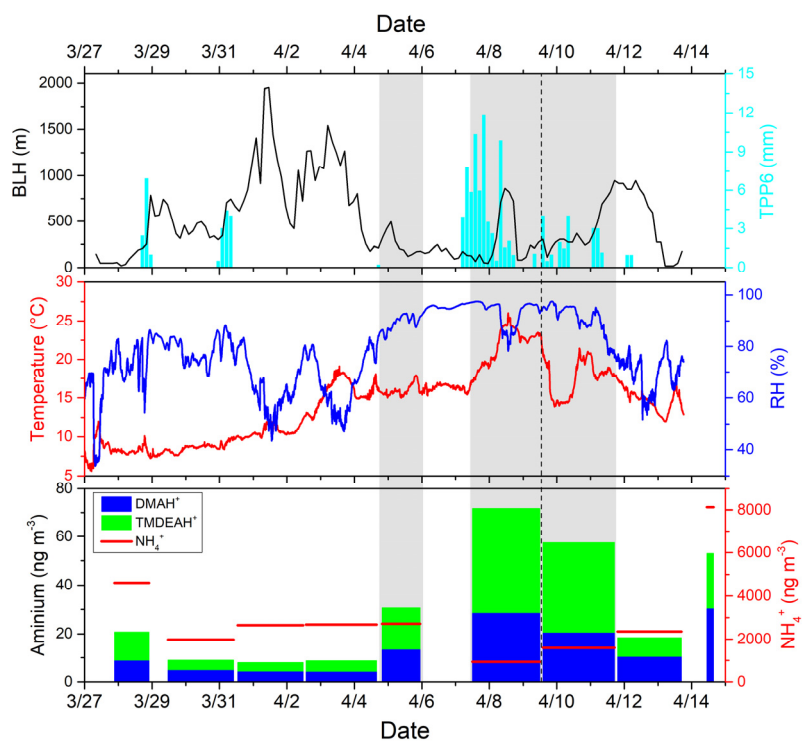
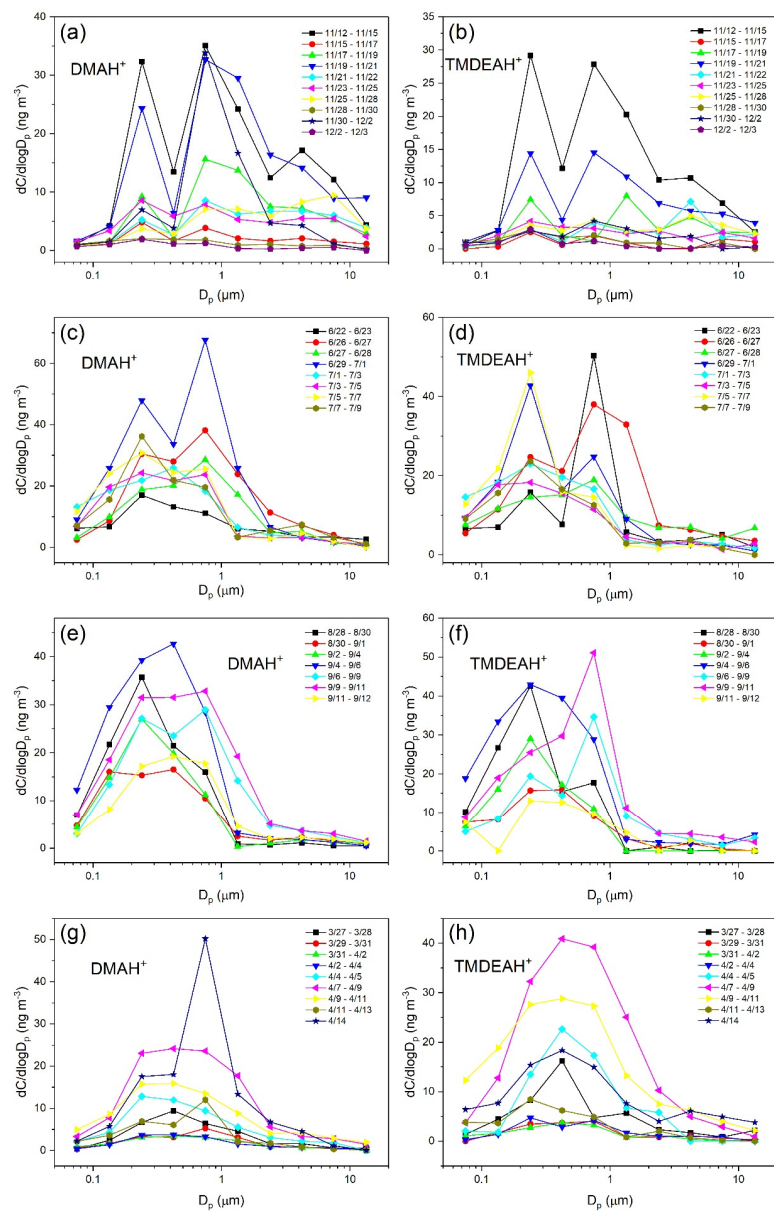


Figure 4. Correlations between concentrations of aminiums and HCOO^- over the Yellow and East China seas (YECS) in the spring of 2017.



704 **Figure 54.** Time series of meteorological parameters and the concentrations of aminiums and NH_4^+ during the cruise of 2017. The time range
705 spanned by the column of each aminium concentration corresponds to the sampling time.



706 **Figure 65.** Size distributions of aminiums during different campaigns. (a-b): in the autumn of 2016 at Huaniao Island, (c-d): in early summer
707 of 2017 at Huaniao Island, (e-f): in late summer of 2017 at Huaniao Island, (g-h): in 2017 spring cruise over the Yellow and East China seas.
708

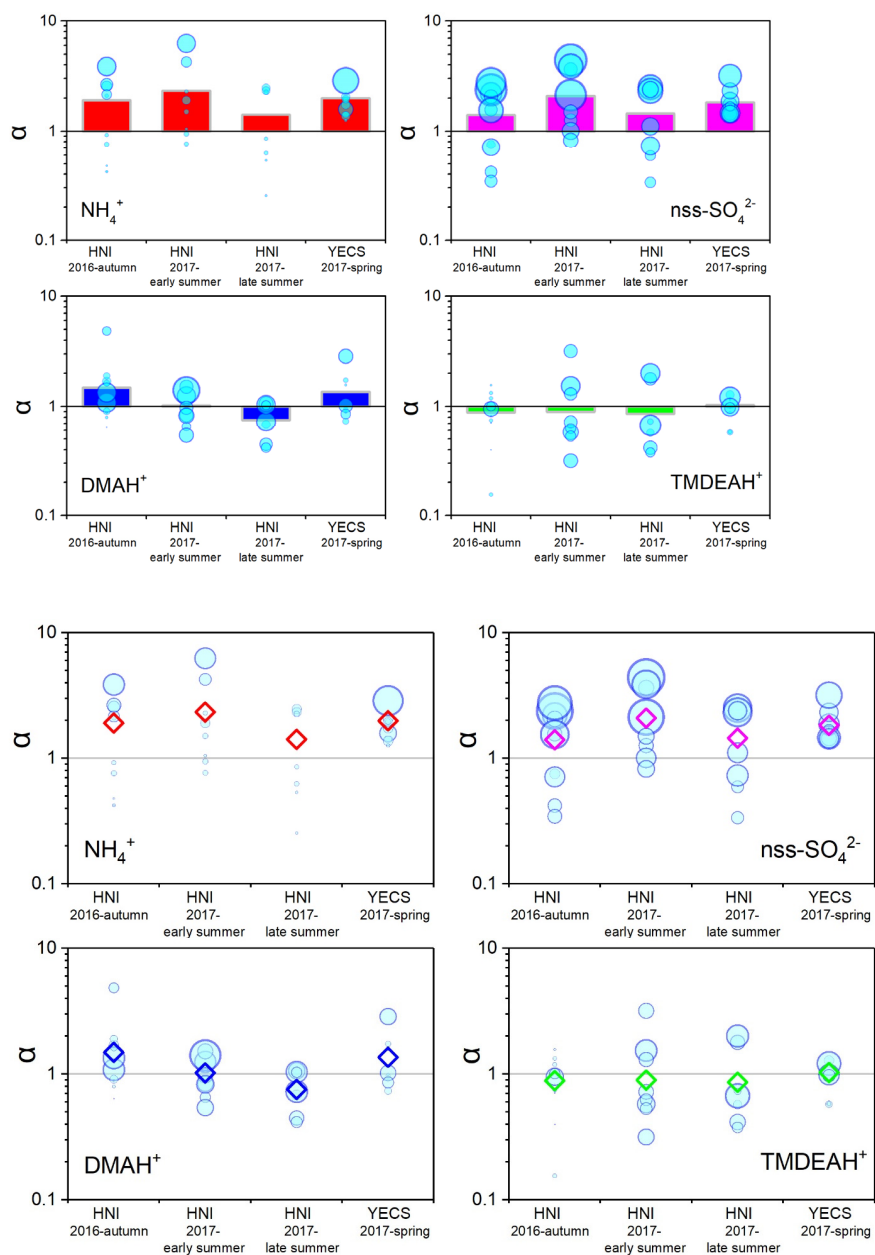


Figure 76. The α values of NH_4^+ , nss-SO_4^{2-} and aminiums in different campaigns. The diameter of the circle is proportional to the concentration and the diamond-shape symbol represents the average value of α for each campaign. It should be noted that the bottom of column is the line of $\alpha=1$.

715
716

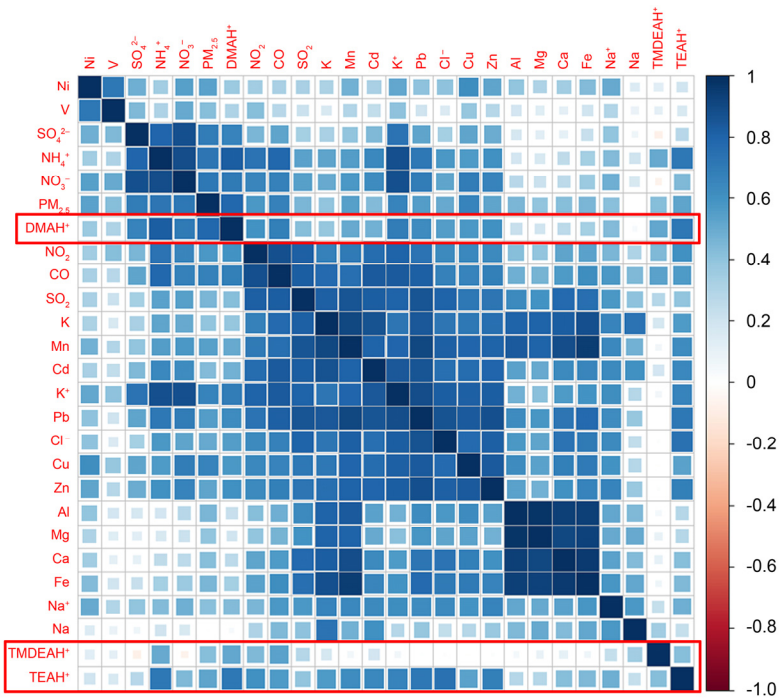


Figure 87. Correlation coefficient matrix among the concentrations of PM_{2.5} components and gaseous pollutants over Shanghai in 2013.

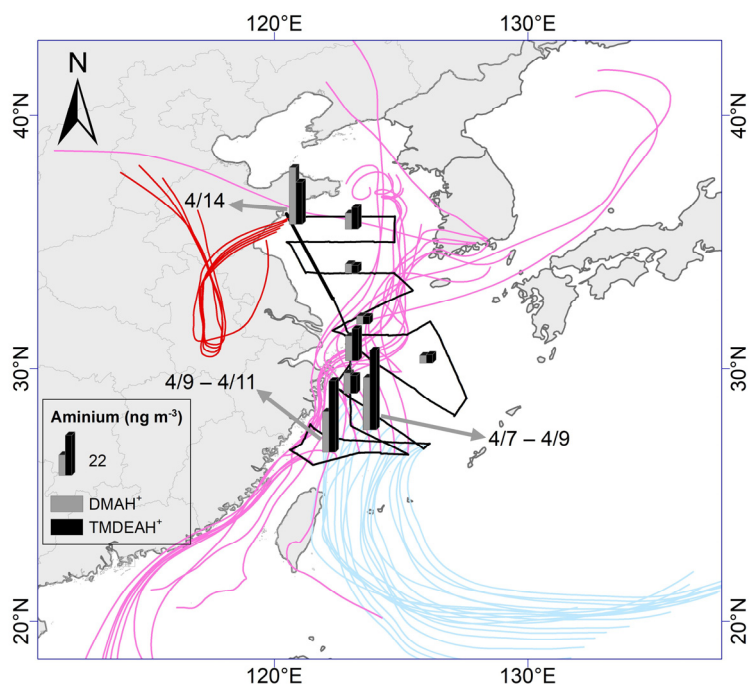


Figure 98. The spatial distribution of aminiums over the YECS in the spring of 2017. The ocean color represents the concentration of chlorophyll a obtained from Kriging interpolation from the observed concentrations. The light blue, pink and red lines represent 72-hour backward trajectories corresponding to sample sets collected on 7–9 Apr., 9–11 Apr. and 14 Apr., respectively.

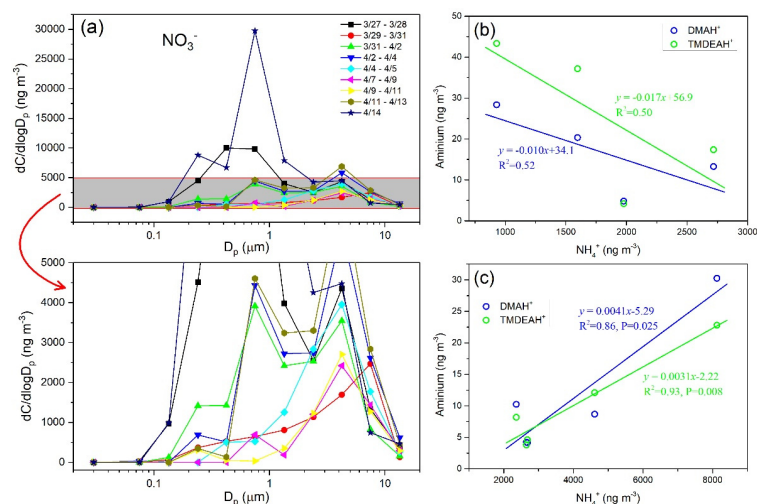


Figure 409. (a) Size distributions of NO_3^- over the YECS in the spring of 2017. (b) Correlations between concentrations of aminiums and NH_4^+ for the samples mainly influenced by marine air masses. (c) Correlations between concentrations of aminiums and NH_4^+ for the samples predominantly influenced by terrestrial transport.

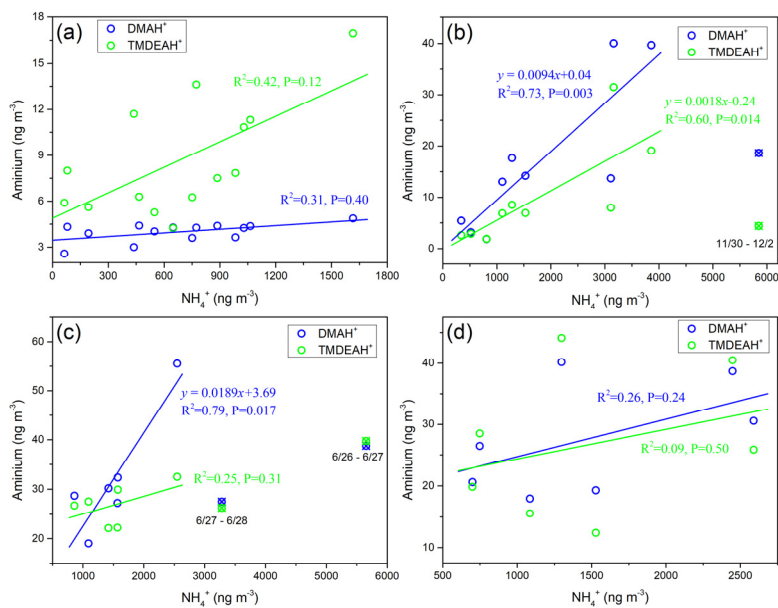


Figure 410. Correlations between ammoniums and NH₄⁺ concentrations over Huaniao Island for each campaign. (a): in the summer of 2016, (b): in the autumn of 2016, (c): in early summer of 2017, (d): in late summer of 2017.

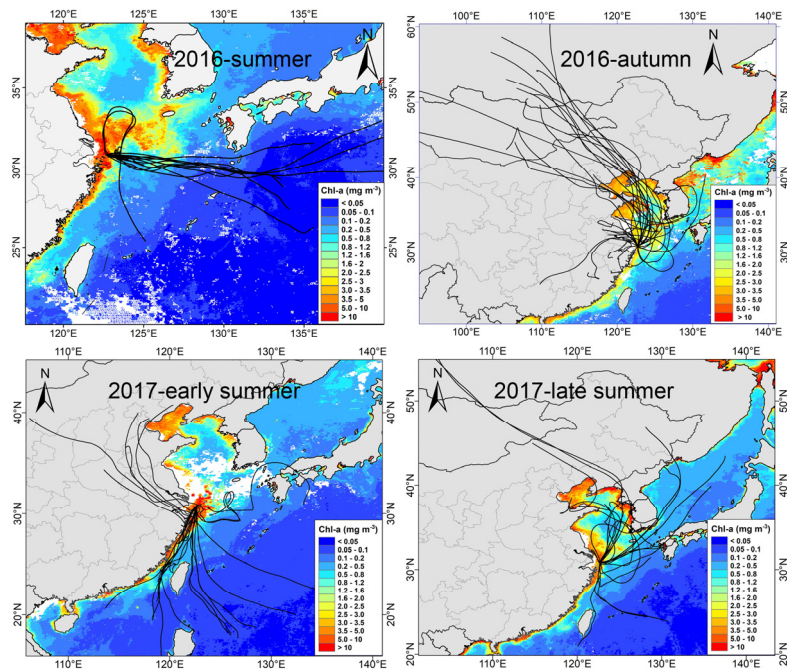
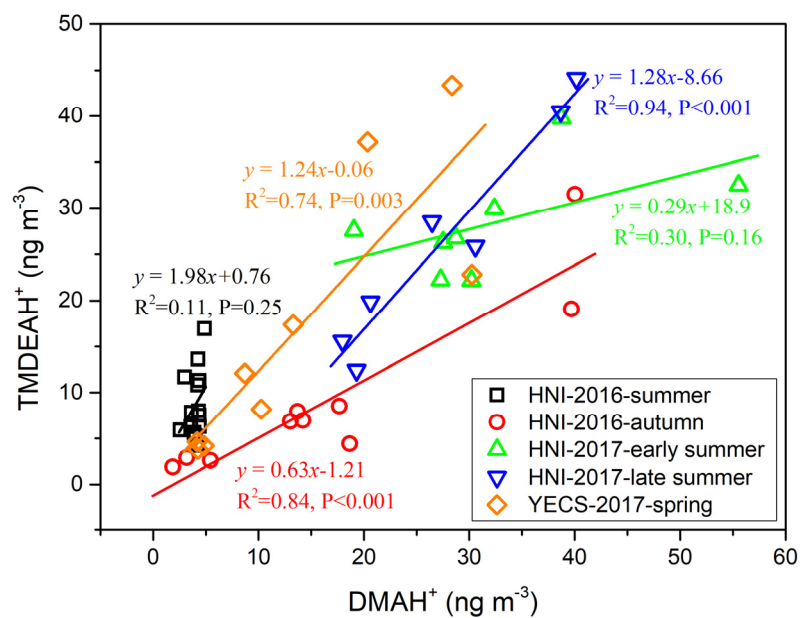
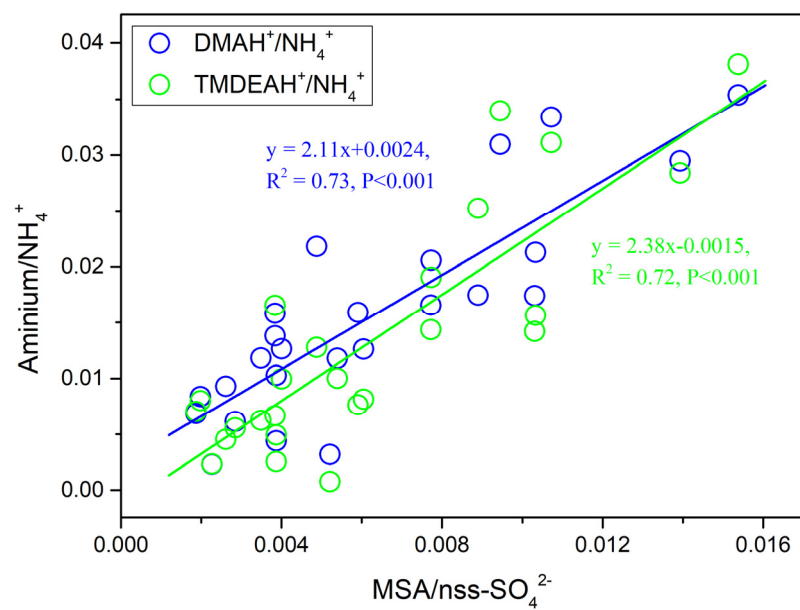


Figure 421. The 72-hour backward trajectories starting from Huaniao Island and the average chlorophyll a concentration retrieved and combined from aqua- and terra-MODIS during the sampling period. Each sample during the summer of 2016 corresponds to one trajectory

731 with a starting time in the middle of sampling period. Each sample set during the autumn of 2016 and the summer of 2017 corresponds to 3
732 trajectories and the starting times are taken at equal intervals in the sampling period.



733
734 **Figure 1412.** Correlations between DMAH^+ and TMDEAH^+ for each campaign over Huaniao Island and the YECS.



735
736 **Figure 1413.** Correlations between aminium/ NH_4^+ and $\text{MSA}/\text{nss-SO}_4^{2-}$ over Huaniao Island during the autumn in 2016 and the summer in
737 2017.

739

Table 1. Summary of sampling information in different campaigns.

Sampling site	Sampler	Sampling period	Number of samples or sample sets
Fudan University, Shanghai	Medium-flow PM _{2.5} sampler	25 Mar. 2013–26 Apr. 2013 (spring)	29
		16 Jul. 2013–17 Aug. 2013 (summer)	26
		30 Oct. 2013–30 Nov. 2013 (autumn)	29
		1 Dec. 2013–23 Jan. 2014 (winter)	47 37
Huaniao Island	Medium-flow PM _{2.5} sampler	4 Aug. 2016–18 Aug. 2016 (summer)	14
Huaniao Island	MOUDI	12 Nov. 2016–3 Dec. 2016 (autumn)	9
		11 Mar. 2017–19 Mar. 2017 (spring)	4
		22 Jun. 2017–9 Jul. 2017 (early summer)	8
		27 Aug. 2017–12 Sep. 2017 (late summer)	7
the Yellow Sea and the East China Sea	MOUDI	27 Mar. 2017–14 Apr. 2017 (spring)	9

批注 [1]: We made a mistake in counting the number of samples and here we have corrected it.

740

741

Table 2. The mass concentrations (mean values \pm 1 standard deviation) of NH_4^+ and aminiums over Shanghai, Huaniao Island and the YECS compared to other sites reported in literatures. The values below the detection limits are indicated by < DL.

No.	Site	Site type	Sampling period	Particle size	NH_4^+ ($\mu\text{g m}^{-3}$)	Aminium (ng m^{-3})					Reference
						MMAH ⁺	DMAH ⁺	TMDEAH ⁺	MEAH ⁺	TEAH ⁺	
1	Shanghai, China	urban	Spring (Mar.–Apr. 2013)	PM _{2.5}	6.0 \pm 3.4		6.4 \pm 6.1	4.8 \pm 2.3		8.4 \pm 8.4	this study
2			Summer (Jul.–Aug. 2013)	PM _{2.5}	3.1 \pm 2.9		9.1 \pm 15.2	1.7 \pm 1.6		0.9 \pm 1.0	
3			Autumn (Nov. 2013)	PM _{2.5}	6.8 \pm 4.5		15.5 \pm 13.4	2.8 \pm 2.9		12.7 \pm 12.2	
4			Winter (Dec. 2013–Jan. 2014)	PM _{2.5}	13.7 \pm 9.8		27.3 \pm 29.0	7.3 \pm 6.2		35.2 \pm 45.6	
5	Shanghai, China	urban	Jul.–Aug. 2013	PM _{1.8}	2.5 \pm 1.3	8.9 \pm 6.1	15.7 \pm 7.9	38.8 \pm 17.0	11.5 \pm 17.4		(Tao et al., 2016)
6				PM ₁₀	2.6 \pm 1.3	9.9 \pm 6.9	20.1 \pm 10.7	47.0 \pm 19.9	15.7 \pm 26.4		
7	Shanghai, China	urban	Jan. 2013	PM _{2.5}		2.4			0.2		(Huang et al., 2016)
8			Jul.–Aug. 2013	PM _{2.5}		3.9			0.3		
9	Yangzhou, China	urban	Nov. 2015–Apr. 2016	PM _{2.5}		4.9 \pm 1.9	4.3 \pm 2.4		15.4 \pm 8.1		(Shen et al., 2017)
10	Nanjing, China	urban	Apr.–May 2016	PM _{2.5}		7.6	4.2		21.7		
11			Aug. 2014	PM _{1.8}		7.2 \pm 4.1	18.0 \pm 11.7		36.4 \pm 18.6		
12	Xi'an, China	urban	Jul. 2008–Aug. 2009	PM _{2.5}		14.4 \pm 9.6			3.3 \pm 2.4		(Ho et al., 2015)
13	Guangzhou, China	urban	Sep.–Oct. 2014	PM _{0.95}	4.3 \pm 1.1	41.8 \pm 11.4	14.5 \pm 3.2	3.7 \pm 0.9	3.2 \pm 0.4		(Liu et al., 2017)
14				PM ₃	5.1 \pm 1.4	50.4 \pm 13.7	17.7 \pm 3.6	4.8 \pm 1.4	4.0 \pm 0.5		
15				PM ₁₀	5.2 \pm 1.4	51.8 \pm 13.9	19.0 \pm 3.8	5.4 \pm 1.6	4.2 \pm 0.6		
16	Tampa Bay, Florida, USA	urban	Jul.–Sep. 2005	PM _{2.5}	1.4 \pm 1.2		31.6 \pm 28.3				(Calderón et al., 2007)
17	a traffic site, Milan, Italy	urban	Oct. 2013	TSP	4.2 \pm 2.9		90 \pm 20			360 \pm 20	(Perrone et al., 2016)
18	a limited traffic site, Milan, Italy	urban	Oct. 2013	TSP	4.0 \pm 3.0		100 \pm 10			420 \pm 100	
19	Qingdao, China	semi-urban	May 2013, Nov.–Dec. 2013, Nov.–Dec. 2015	PM _{0.056-10}			6.3	5.8			(Xie et al., 2018)
20	resort beach site of Qingdao, China	coastal, rural	Aug. 2016	PM _{0.056-10}			28.5 \pm 23.0	9.0 \pm 6.6			
21	Egbert, Toronto, Canada	agricultural and semi-forested	Oct. 2010	PM _{2.5}			0.1 \pm 0.2	1 \pm 0.6			(VandenBoer et al., 2012)
22	Hyytiälä, southern Finland	boreal forest	Mar. 2015	PM ₁₀	0.4 \pm 0.1	6.8	1.5	1.1			(Hemmilä et al., 2018)
23			Apr. 2015	PM ₁₀	0.1 \pm 0.1	2.9	3.1	0.7			
24			Jul. 2015	PM ₁₀	0.1 \pm 0.1	3.0	8.4 \pm 4.9	1.8 \pm 1.4	0.4		
25	Nanling, Guangdong, China	forest	Oct. 2016	PM _{2.5}	0.9 \pm 0.6	8.8 \pm 7.8	2.4 \pm 3.2	1.1 \pm 1.8			(Liu et al., 2018a)
26			May–Jun. 2017		1.8 \pm 1.6	11.9 \pm 9.8	5.0 \pm 2.2	1.7 \pm 1.7			

No.	Site	Site type	Sampling period	Particle size	NH ₄ ⁺ (μg m ⁻³)	Aminium (ng m ⁻³)					Reference
						MMAH ⁺	DMAH ⁺	TMDEAH ⁺	MEAH ⁺	TEAH ⁺	
27	Brent, Alabama, USA	forest	Jun.1 – July 15, 2013	submicron	0.52	148*					(You et al., 2014)
28	Huaniao Island, China	marine	Aug. 2016	PM _{2.5}	0.7±0.4		4.0±0.6	8.7±3.7		< DL	this study
29			Nov.–Dec. 2016	PM _{1.8}	1.9±1.5		10.7±9.3	6.0±6.8		< DL	
30				PM ₁₀	2.1±1.8		15.1±12.4	8.4±8.8		< DL	
31			Mar. 2017	PM _{1.8}	2.0±1.2		6.8±4.6	2.7±1.8		< DL	
32				PM ₁₀	2.3±1.4		11.4±11.6	3.1±2.2		< DL	
33			Jun.–Jul. 2017	PM _{1.8}	2.1±1.4		29.0±10.8	24.8±5.4		< DL	
34				PM ₁₀	2.2±1.6		32.2±11.0	27.5±5.7		< DL	
35			Aug.–Sep. 2017	PM _{1.8}	1.4±0.7		25.8±8.7	25.0±11.0		< DL	
36				PM ₁₀	1.5±0.8		27.4±9.1	26.3±11.6		< DL	
37	the Yellow Sea and the East China Sea	marine	Mar.–Apr. 2017	PM _{1.8}	2.8±2.0		11.9±9.0	14.6±12.9		< DL	
38				PM ₁₀	3.0±2.2		13.5±10.1	16.6±14.5		< DL	
39	the Yellow Sea and the northwest Pacific	marine	Apr. 2015	PM _{0.056-10}			12.9±10.6	13.2±13.8			(Xie et al., 2018)
40	the East China Sea	marine	Jan. 2016	PM _{0.056-10}			30.8±9.7	12.0±6.6			
41	the Yellow Sea and the Bohai Sea	marine	Aug. 2015, Jun.–Jul. 2016	PM _{0.056-10}			33.3	19.4			
42	the south Yellow Sea	marine	Nov. 2013	PM _{0.056-10}			18.9±16.6	31.8±19.2			
43	the Yellow Sea and the Bohai Sea	marine	May 2012	PM ₁₁			202±170	432±426			(Hu et al., 2015)
44	the south Yellow Sea	marine	Nov. 2012	PM ₁₀			13.3±4.6	30.0±12.6			(Yu et al., 2016)
45	the north Yellow Sea and the Bohai Sea	marine	Nov. 2012	PM ₁₀			-	15.0±6.6			
46	Arabian Sea	marine	Aug.–Oct. 1994	PM _{0.9}	0.04	3.2	2.1	0.3			(Gibb et al., 1999)
47			Nov.–Dec. 1994	PM _{0.9}	0.1	3.7	11.1	0.5			
48	Mace Head, Ireland	marine	Jan.–Dec. 2006	PM ₁			4.7±6.0	7.6±9.4			(Facchini et al., 2008)
49	Irish West Coast	marine	Jun.–Jul. 2006	PM ₁			14.7±14.3	14.3±8.7			
50	São Vicente, Cape Verde	marine	May–Jun., Dec. 2007	PM _{0.14-0.42}	0.1	0.1	0.4	0.2			(Müller et al., 2009)
51	off the Central Coast of California, USA	marine	Jul. 2007	PM ₁				22			(Sorooshian et al., 2009)
52	the Eastern Mediterranean, Greece	marine	2005–2006	PM ₁			9.2±36.8	< DL			(Violaki and Mihalopoulos, 2010)

* Fourier Transform Infrared spectroscopy (FTIR) measured total primary aminiums (R-NH₃⁺)

745 **Table 3.** Calculated terrestrial and marine source contributions to aerosol aminiums over Huaniao Island. (mean (minimum –
746 maximum)).

Campaign	DMAH ⁺		TMDEAH ⁺	
	Terrestrial contribution (%)	Marine contribution (%)	Terrestrial contribution (%)	Marine contribution (%)
2016-autumn	71.2 (59.6 - 81.9) 74.1 (42.5 - 100)	28.8 (18.1 - 40.4) 25.9 (0 - 57.5)	61.6 (25.6 - 87.4) 34.3 (0 - 100)	38.4 (12.6 - 74.3) 65.7 (0 - 100)
2017-early summer	42.6 (30.5 - 54.7) 20.3 (0 - 98.8)	57.3 (45.3 - 69.5) 1.2 (0 - 79.7)	20.9 (5.8 - 39.1) 11.0 (0 - 48.6)	79.1 (12.6 - 94.7) 89.0 (0 - 100)
2017-late summer	33.8 (24.3 - 45) 19.2 (0 - 57.4)	66.2 (54.3 - 75) 12.8 (0 - 80.8)	17.5 (4.2 - 32.9) 9.0 (0 - 42.1)	82.5 (67.1 - 95.4) 78.3 (57.9 - 91.0)

Total suspended particle (TSP) sample collection and measurement

TSP samples were collected at Huaniao Island during the autumn of 2016 (24 Oct. – 1 Dec.) and the summer of 2017 (21 Jun. – 9 Jul. and 28 Aug. – 12 Sep.) by a high-volume sampler (1050 L min⁻¹, HY-1000D, Hengyuan) using cellulose filters. The sampling duration was commonly 24 hours. 1/32 of TSP sample filter was cut and extracted ultrasonically by 20 mL of ultrapure water (18.25 MΩ cm⁻¹). The extract was then filtered and analyzed for anions using Ion Chromatograph.

Calculation of the retention percentage of air mass over the land (R_L)

The three-day backward trajectories starting from Huaniao Island were calculated every 3 hours for each TSP sample (Figure S9). There are a total of 73 endpoints tracking 0 to 72 hours along each trajectory, and then the proportion of endpoints over the land was calculated. In addition, the regions corresponding to longer backward tracking time had weaker influence on the receptor site than the nearby regions, so a weighting factor associated with the backward tracking time was also included. The calculation is shown as below.

$$R_L = \frac{\sum_{i=1}^{N_{land}} e^{-\frac{t_i}{72}}}{\sum_{i=1}^{N_{total}} e^{-\frac{t_i}{72}}} \times 100\%$$

where N_{total} is the total number of trajectory endpoints corresponding to a TSP sample. N_{land} is the total number of trajectory endpoints located over the land. t_i is the backward tracking time with the unit of hour and $e^{-\frac{t_i}{72}}$ is the weighting factor.

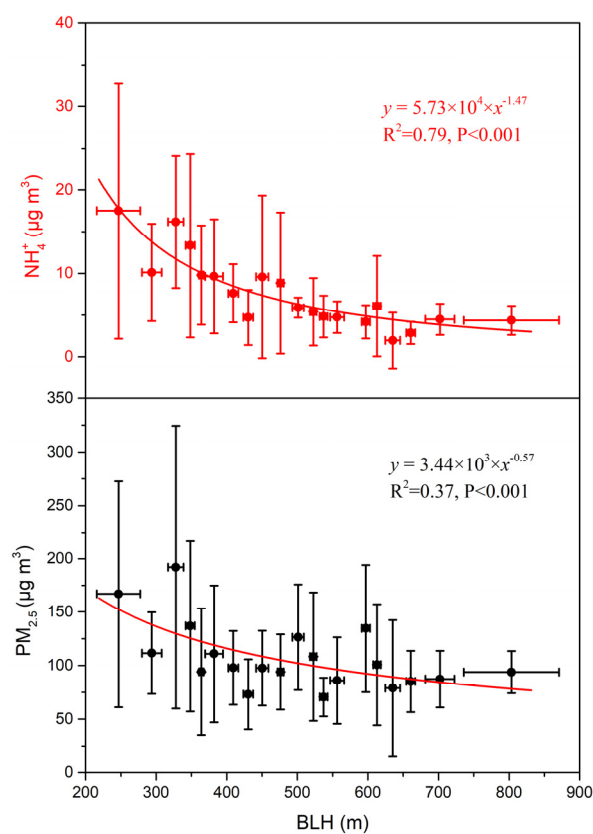


Figure S1. Relationships between concentrations of $\text{PM}_{2.5}$ and NH_4^+ and boundary layer height (BLH).

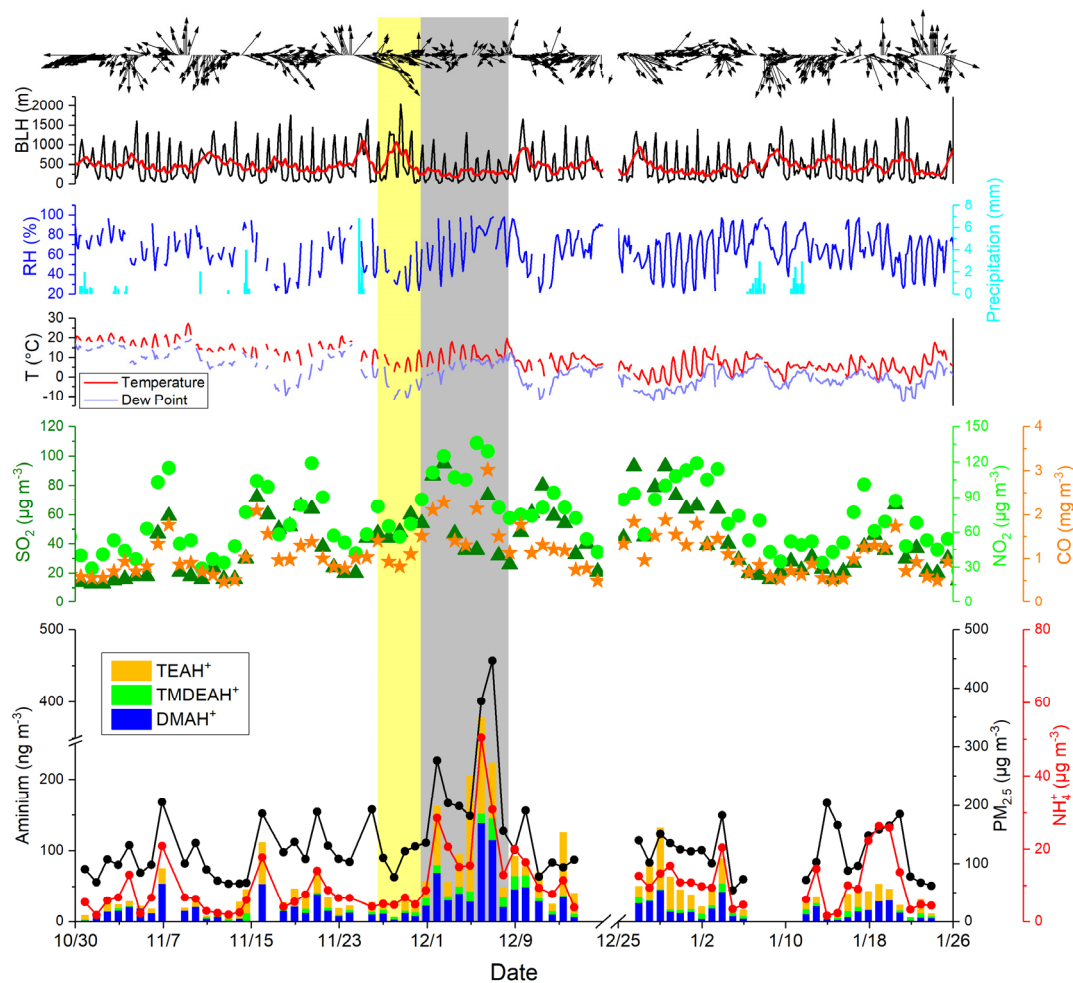


Figure S2. Time series of concentrations of atmospheric species and meteorological factors during the autumn and winter of 2013 in Shanghai.

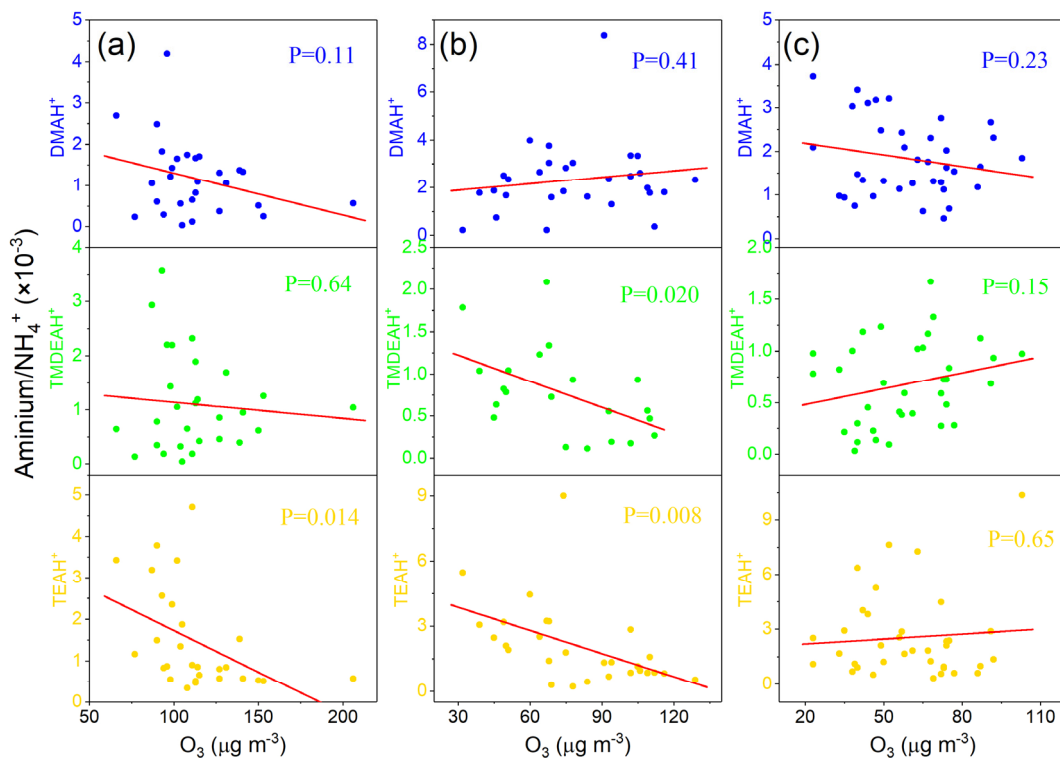


Figure S3. Relationships between mass ratios of aminiums to NH_4^+ and O_3 concentrations over Shanghai in the (a) spring, (b) autumn and (c) winter of 2013.

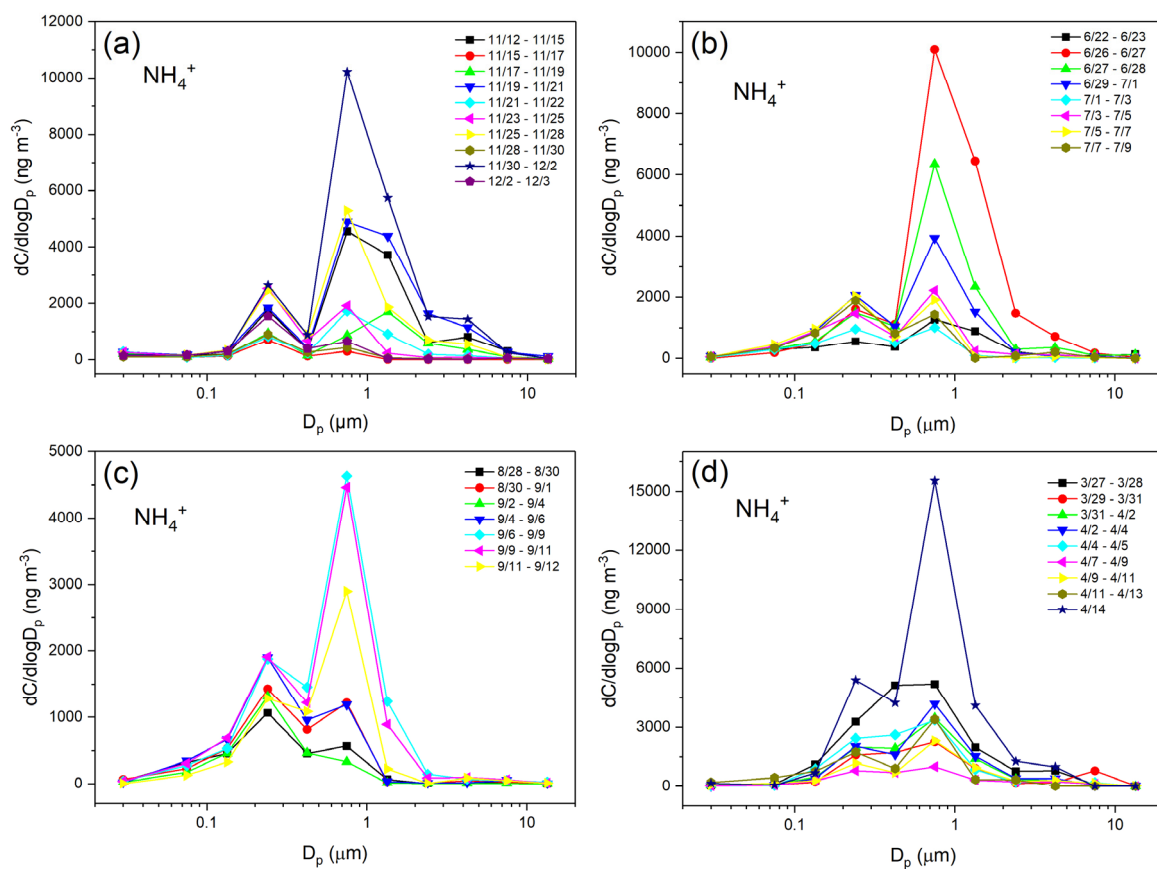


Figure S3S4. Size distributions of NH_4^+ during different campaigns. (a): in the autumn of 2016 at Huaniao Island, (b): in early summer of 2017 at Huaniao Island, (c): in late summer of 2017 at Huaniao Island, (d): in 2017 spring cruise over the Yellow and East China seas.

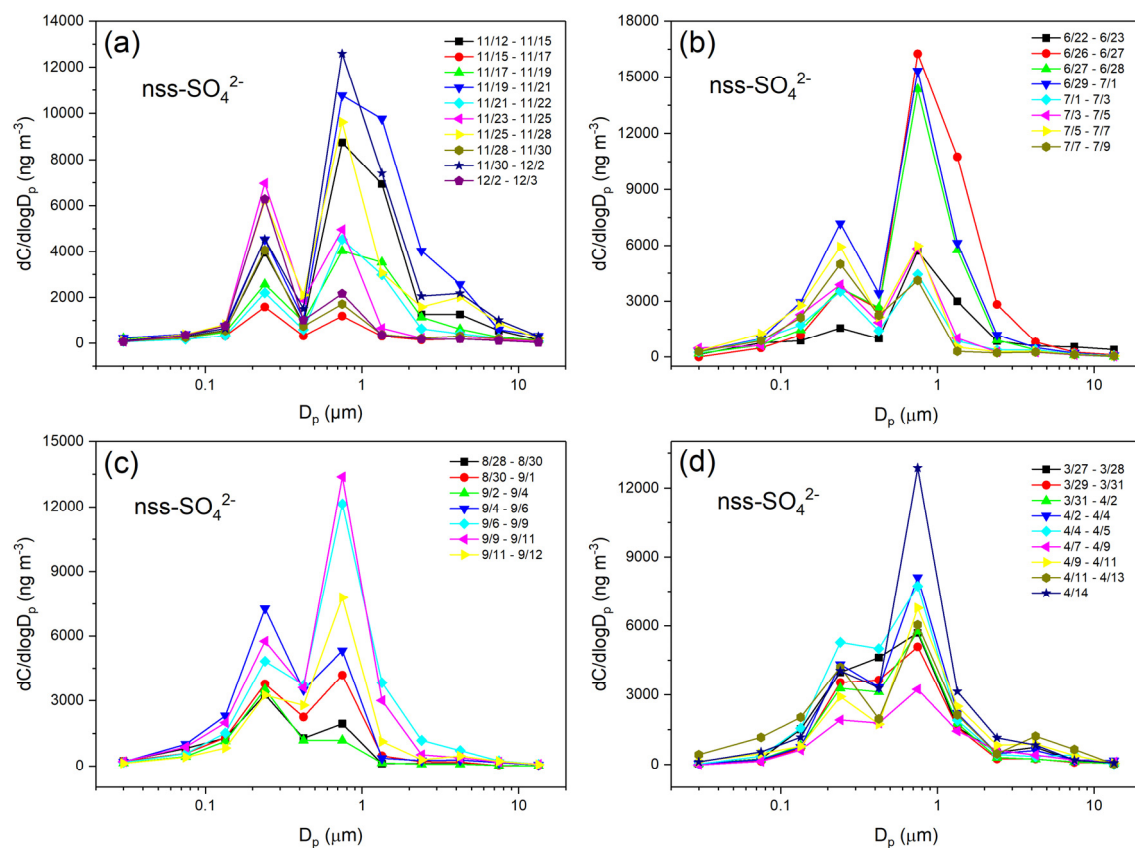


Figure S4S5. Size distributions of nss-SO_4^{2-} during different campaigns. **(a):** in the autumn of 2016 at Huaniao Island, **(b):** in early summer of 2017 at Huaniao Island, **(c):** in late summer of 2017 at Huaniao Island, **(d):** in 2017 spring cruise over the Yellow and East China seas.

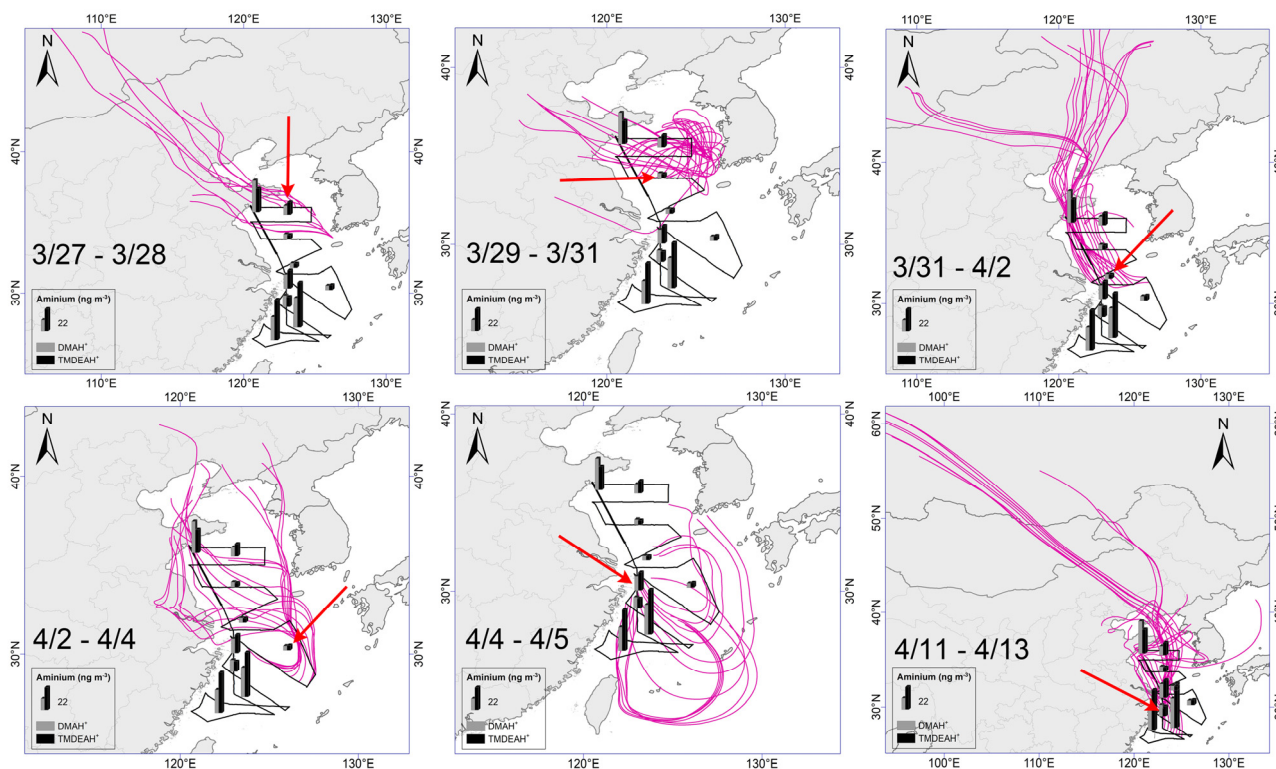


Figure S5S6. 72-hour air mass backward trajectories for the samples other than those were plotted in Figure 9.

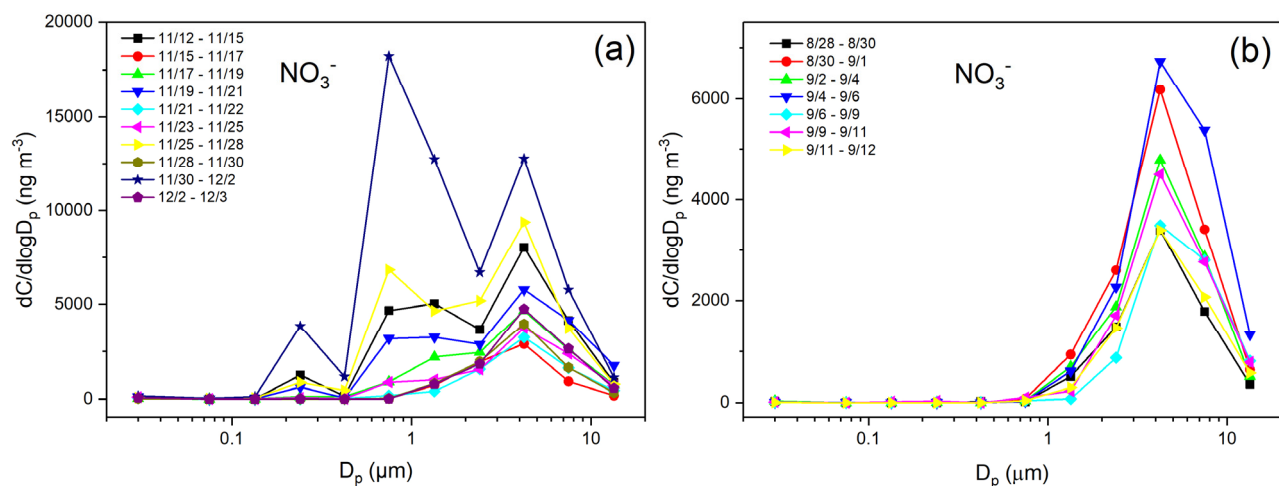


Figure S6S7. (a) Size distributions of NO_3^- over Huaniao Island in the autumn of 2016. (b) Size distributions of NO_3^- over Huaniao Island in the late summer of 2017.

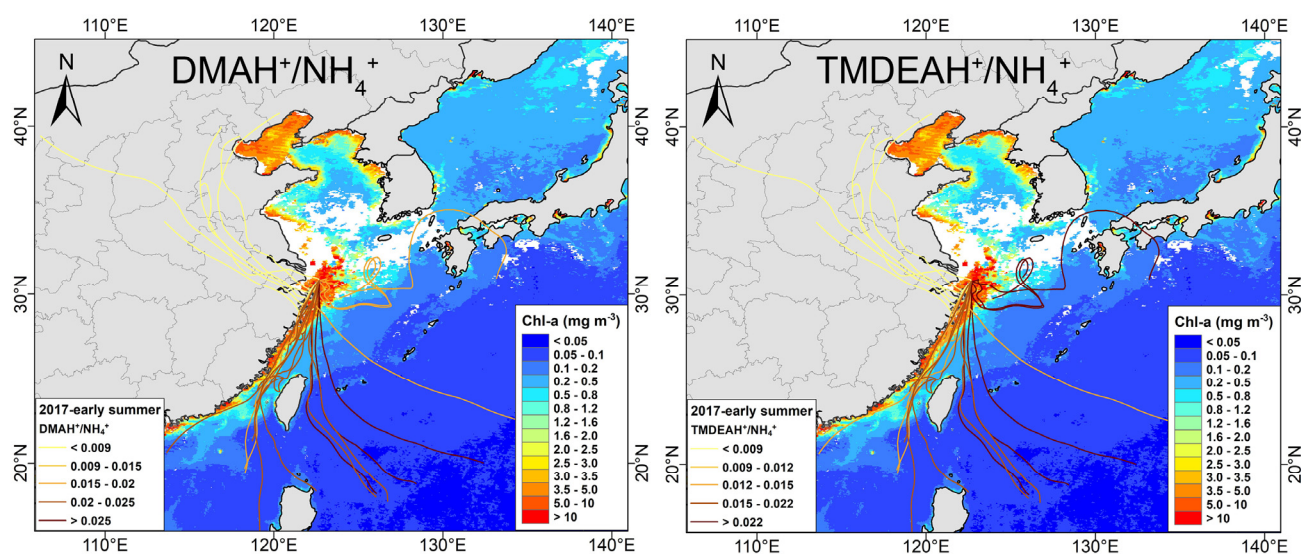


Figure S7S8. The backward trajectories starting from Huaniao Island during early summer in 2017 and the mass ratio of aminium to NH_4^+ for the corresponding sample.

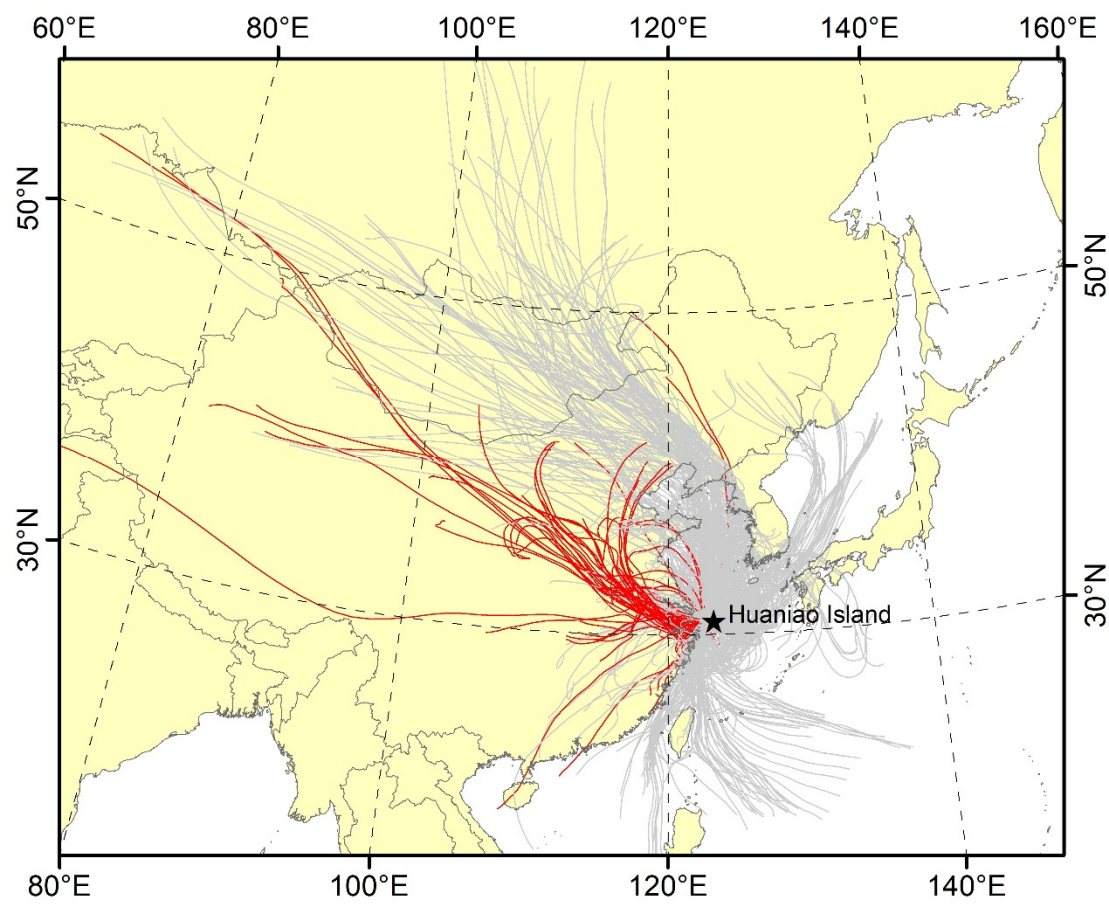


Figure S9. The three-day backward trajectories starting from Huaniao Island during the autumn of 2016 and the summer of 2017 corresponding to TSP samples. A new trajectory was calculated every 3 hours during the sampling period of each sample. The red trajectories corresponded to the samples identified as terrestrial dominated.